

March 13, 2019 | SIAM-GS 2019, Houston, TX, USA

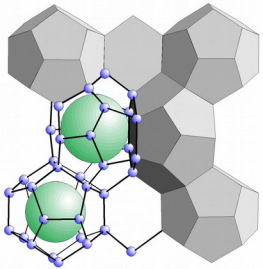
# Modelling Coupled Phase Transitions in Gas Hydrate Geosystems

Shubhangi Gupta<sup>\*,1</sup>, Barbara Wohlmuth<sup>2</sup>, and Matthias Haeckel<sup>1</sup>

<sup>1</sup>GEOMAR Helmholtz Center for Ocean Research Kiel

<sup>2</sup>Technical University of Munich

# Gas Hydrates

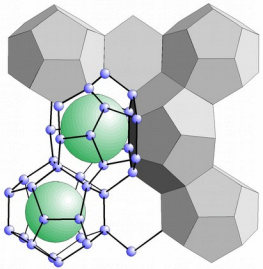


gas  
H<sub>2</sub>O

Image source: J.Greinert, Geomar

- Gas hydrate → ice-like solid, immobile(?)

# Gas Hydrates



gas  
H<sub>2</sub>O

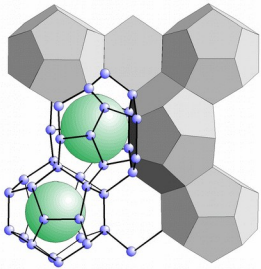


Methane  
hydrate

Image source: J.Greinert, Geomar

- Gas hydrate → ice-like solid, immobile(?)

# Gas Hydrates

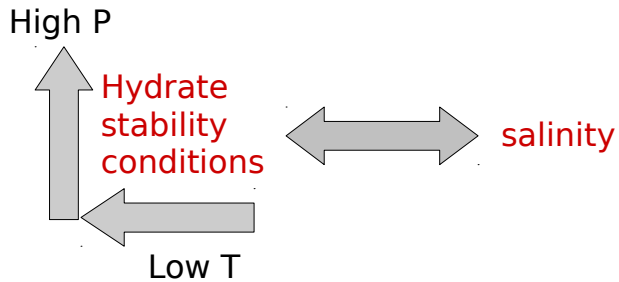


gas  
H<sub>2</sub>O



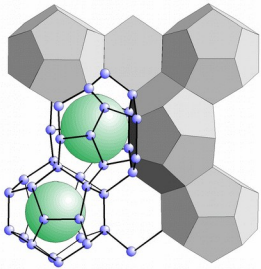
Methane  
hydrate

Image source: J.Greinert, Geomar



- Gas hydrate → ice-like solid, immobile(?)
- Stable at high P, lo T
- Extremely sensitive to local thermodynamic state (P,T,salinity...)

# Gas Hydrates

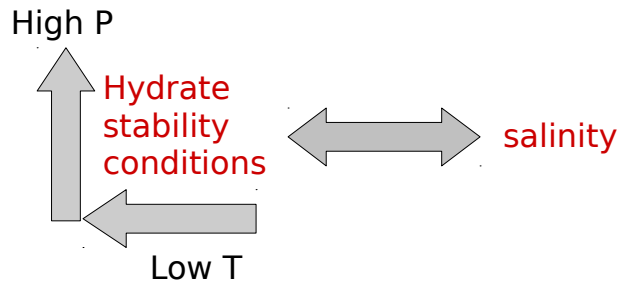


gas  
H<sub>2</sub>O



Methane  
hydrate

Image source: J.Greinert, Geomar



- Gas hydrate → ice-like solid, immobile(?)
- Stable at high P, lo T
- Extremely sensitive to local thermodynamic state (P,T,salinity...)

## Challenges in modelling marine gas hydrates

- Predominantly **water saturated** domains
- environmental changes can locally destabilize hydrates
- **Free gas signatures as low as 0.5%!**
- Strong influence of salinity, **dilution effects**

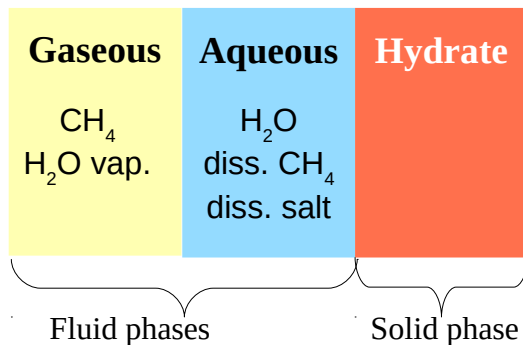
# Mathematical Model

## Four main components

$\text{CH}_4$  ,  $\text{H}_2\text{O}$  , Hydrate , Dissolved salt

## Three phases

Gaseous, Aqueous, Solid



# Mathematical Model

## Four main components

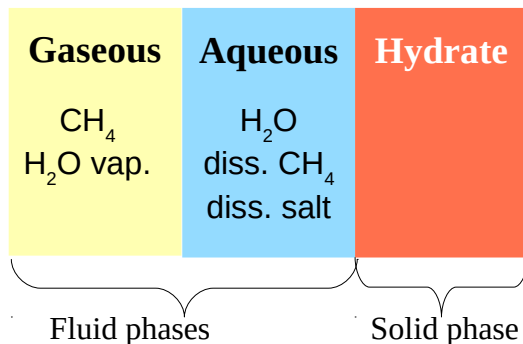
$\text{CH}_4$  ,  $\text{H}_2\text{O}$  , Hydrate , Dissolved salt

## Three phases

Gaseous, Aqueous, Solid

## Model considers:

- Multi-phase, multi-component flow
- $\text{CH}_4 \leftrightarrow \text{H}_2\text{O}$  VLE
- Hydrate phase change
- Thermal effects due hydrate phase change



# Mathematical Model

## Four main components

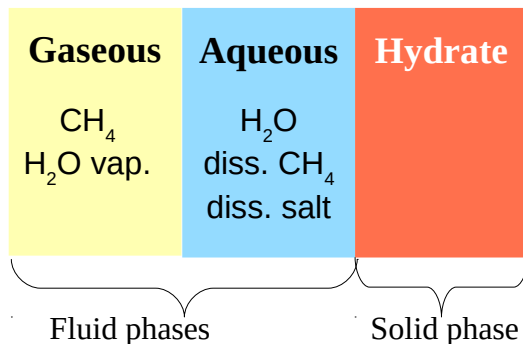
$\text{CH}_4$  ,  $\text{H}_2\text{O}$  , Hydrate , Dissolved salt

## Three phases

Gaseous, Aqueous, Solid

## Model considers:

- Multi-phase, multi-component flow
- $\text{CH}_4 \leftrightarrow \text{H}_2\text{O}$  VLE  $\longrightarrow$  eqb. Phase transition
- Hydrate phase change  $\longrightarrow$  kinetic phase transition
- Thermal effects due hydrate phase change





# Mathematical Model

## Four main components

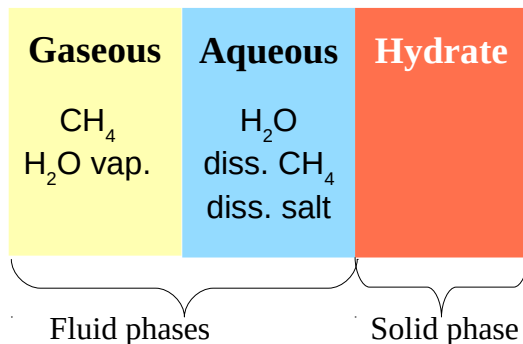
CH<sub>4</sub> , H<sub>2</sub>O , Hydrate , Dissolved salt

## Three phases

Gaseous, Aqueous, Solid

## Model considers:

- Multi-phase, multi-component flow
- CH<sub>4</sub> ↔ H<sub>2</sub>O VLE
- Hydrate phase change
- Thermal effects due hydrate phase change



## Governing equations

Mass balance for mobile components  $\kappa = CH_4, H_2O$ :

$$\Sigma_{\alpha} (\partial_t \phi \rho_{\alpha} S_{\alpha} \chi_{\alpha}^{\kappa}) + \Sigma_{\alpha} (\nabla \cdot \rho_{\alpha} \chi_{\alpha}^{\kappa} \mathbf{v}_{\alpha}) = \Sigma_{\alpha} (\nabla \cdot \phi S_{\alpha} \mathbf{J}_{\alpha}^{\kappa}) + \dot{g}^{\kappa}$$

where,  $\mathbf{v}_{\alpha} = -K \frac{k_{r,\alpha}}{\mu_{\alpha}} (\nabla P_{\alpha} - \rho_{\alpha} \mathbf{g})$  and  $\mathbf{J}_{\alpha}^{\kappa} = -\tau D_{\alpha}^{\kappa} (\rho_{\alpha} \nabla \chi_{\alpha}^{\kappa})$

Mass balance for hydrate phase:

$$\partial_t \phi \rho_h S_h = \dot{g}_h$$

Mass balance for dissolved salt:

$$\partial_t \phi \rho_w S_w \chi_w^c + \nabla \cdot \rho_w \chi_w^c \mathbf{v}_w = \nabla \cdot \phi S_w \mathbf{J}_w^c$$

Energy balance:

$$\partial_t [(1-\phi) \rho_s u_s + \Sigma_{\beta} \phi \rho_{\beta} S_{\beta} u_{\beta}] + \Sigma_{\beta} \nabla \cdot (\phi \rho_{\beta} S_{\beta} \mathbf{v}_{\beta,t} h_{\beta}) = \nabla \cdot (-k_{eff}^{th} \nabla T) + \dot{Q}_h$$

## Closure relations

summation condition for  $\beta = g, w, h$  :  $\Sigma_{\beta} S_{\beta} = 1$

and, relation between fluid pressures:  $P_g - P_w = P_c(S_w, S_h, \phi \dots)$

$$g^{\dot{C}H_4} + g^{\dot{H}_2O} + \dot{g}_h = 0 \quad \text{and} \quad \forall \alpha = g, w, \quad \Sigma_{\kappa} \mathbf{J}_{\alpha}^{\kappa} = 0$$

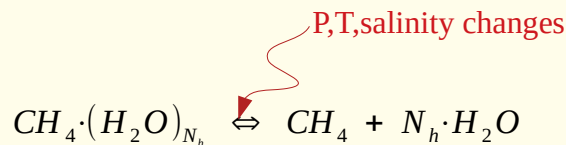
## Hydraulic properties

$$K = K_0 \cdot f_{S_h}^K(S_h) , \quad P_c = P_c^{BC}(S_{we}) \cdot f_{S_h}^{P_c}(S_h)$$

# Mathematical Model

## Two main phase transitions

### 1. non-equilibrium hydrate phase change



$$\dot{g}_g = k_{reac} A_{rs} (P_g - P_{eqb})$$

$$\text{where, } P_{eqb} = f(T, \chi_w^c),$$

$$k_{reac} = k_{reac}^0 \exp\left(-\frac{\Delta E_a}{T}\right), \text{ and } A_{rs} = A_{rs}(S_h, \phi, K)$$

## Governing equations

Mass balance for mobile components  $\kappa = CH_4, H_2O$ :

$$\Sigma_{\alpha} (\partial_t \phi \rho_{\alpha} S_{\alpha} \chi_{\alpha}^{\kappa}) + \Sigma_{\alpha} (\nabla \cdot \rho_{\alpha} \chi_{\alpha}^{\kappa} \mathbf{v}_{\alpha}) = \Sigma_{\alpha} (\nabla \cdot \phi S_{\alpha} \mathbf{J}_{\alpha}^{\kappa}) + \dot{g}^{\kappa}$$

where,  $\mathbf{v}_{\alpha} = -K \frac{k_{r,\alpha}}{\mu_{\alpha}} (\nabla P_{\alpha} - \rho_{\alpha} \mathbf{g})$  and  $\mathbf{J}_{\alpha}^{\kappa} = -\tau D_{\alpha}^{\kappa} (\rho_{\alpha} \nabla \chi_{\alpha}^{\kappa})$

Mass balance for hydrate phase:

$$\partial_t \phi \rho_h S_h = \dot{g}_h$$

Mass balance for dissolved salt:

$$\partial_t \phi \rho_w S_w \chi_w^c + \nabla \cdot \rho_w \chi_w^c \mathbf{v}_w = \nabla \cdot \phi S_w \mathbf{J}_w^c$$

Energy balance:

$$\partial_t [(1-\phi) \rho_s u_s + \Sigma_{\beta} \phi \rho_{\beta} S_{\beta} u_{\beta}] + \Sigma_{\beta} \nabla \cdot (\phi \rho_{\beta} S_{\beta} \mathbf{v}_{\beta,t} h_{\beta}) = \nabla \cdot (-k_{eff}^{th} \nabla T) + \dot{Q}_h$$

## Closure relations

summation condition for  $\beta = g, w, h$  :  $\Sigma_{\beta} S_{\beta} = 1$

and, relation between fluid pressures:  $P_g - P_w = P_c(S_w, S_h, \phi \dots)$

$$g^{\dot{C}H_4} + g^{\dot{H}_2O} + \dot{g}_h = 0 \quad \text{and} \quad \forall \alpha = g, w, \quad \Sigma_{\kappa} \mathbf{J}_{\alpha}^{\kappa} = 0$$

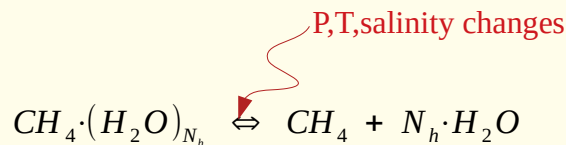
## Hydraulic properties

$$K = K_0 \cdot f_{S_h}^K(S_h), \quad P_c = P_c^{BC}(S_{we}) \cdot f_{S_h}^{P_c}(S_h)$$

# Mathematical Model

## Two main phase transitions

### 1. non-equilibrium hydrate phase change



$$\dot{g}_g = k_{reac} A_{rs} (P_g - P_{eqb})$$

$$\text{where, } P_{eqb} = f(T, \chi_w^c),$$

$$k_{reac} = k_{reac}^0 \exp\left(-\frac{\Delta E_a}{T}\right), \text{ and } A_{rs} = A_{rs}(S_h, \phi, K)$$

### 2. Equilibrium fluid phase changes (VLE)

$$\sum_{\kappa} \chi_{\alpha}^{\kappa} \leq 1 \quad \forall \alpha \quad \text{and} \quad \sum_{\kappa} \chi_{\alpha}^{\kappa} = 1 \quad \text{iff} \quad S_{\alpha} > 0$$

We can cast these inequality constraints as KKT complementarity conditions:

$$1 - \sum_{\kappa} \chi_{\alpha}^{\kappa} \geq 0, \quad S_{\alpha} \geq 0, \quad S_{\alpha} (1 - \sum_{\kappa} \chi_{\alpha}^{\kappa}) = 0.$$

## Governing equations

Mass balance for mobile components  $\kappa = CH_4, H_2O$ :

$$\sum_{\alpha} (\partial_t \phi \rho_{\alpha} S_{\alpha} \chi_{\alpha}^{\kappa}) + \sum_{\alpha} (\nabla \cdot \rho_{\alpha} \chi_{\alpha}^{\kappa} \mathbf{v}_{\alpha}) = \sum_{\alpha} (\nabla \cdot \phi S_{\alpha} \mathbf{J}_{\alpha}^{\kappa}) + \dot{g}^{\kappa}$$

$$\text{where, } \mathbf{v}_{\alpha} = -K \frac{k_{r,\alpha}}{\mu_{\alpha}} (\nabla P_{\alpha} - \rho_{\alpha} \mathbf{g}) \quad \text{and} \quad \mathbf{J}_{\alpha}^{\kappa} = -\tau D_{\alpha}^{\kappa} (\rho_{\alpha} \nabla \chi_{\alpha}^{\kappa})$$

Mass balance for hydrate phase:

$$\partial_t \phi \rho_h S_h = \dot{g}_h$$

Mass balance for dissolved salt:

$$\partial_t \phi \rho_w S_w \chi_w^c + \nabla \cdot \rho_w \chi_w^c \mathbf{v}_w = \nabla \cdot \phi S_w \mathbf{J}_w^c$$

Energy balance:

$$\partial_t [(1-\phi)\rho_s u_s + \sum_{\beta} \phi \rho_{\beta} S_{\beta} u_{\beta}] + \sum_{\beta} \nabla \cdot (\phi \rho_{\beta} S_{\beta} \mathbf{v}_{\beta,t} h_{\beta}) = \nabla \cdot (-k_{eff}^{th} \nabla T) + \dot{Q}_h$$

## Closure relations

summation condition for  $\beta = g, w, h$ :  $\sum_{\beta} S_{\beta} = 1$

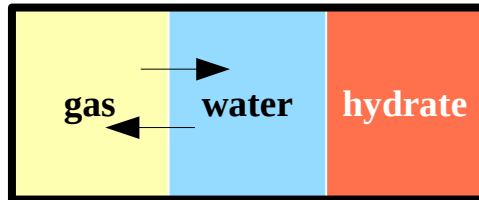
and, relation between fluid pressures:  $P_g - P_w = P_c(S_w, S_h, \phi \dots)$

$$g^{\dot{C}H_4} + g^{\dot{H}_2O} + \dot{g}_h = 0 \quad \text{and} \quad \forall \alpha = g, w, \quad \sum_{\kappa} \mathbf{J}_{\alpha}^{\kappa} = 0$$

## Hydraulic properties

$$K = K_0 \cdot f_{S_h}^K(S_h), \quad P_c = P_c^{BC}(S_{we}) \cdot f_{S_h}^{P_c}(S_h)$$

## Mathematical Model

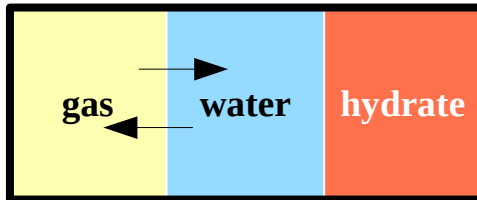


### NUMERICAL SOLUTION

- Fully implicit cell centered finite volume method based discretization  
two-point finite difference flux approximation  
fully upwinded convective fluxes
- Nonlinear **Complementary Constraints** for vanishing gas phase, [Lauser,2011]
- **Semismooth Newton**'s method for Linearization,  
**Active-sets strategy**
- **SuperLU** Linear Solver

Implementation in **DUNE-PDElab** framework  
[Bastian2010]  
(<http://www.dune-project.org>)

# Mathematical Model



## NUMERICAL SOLUTION

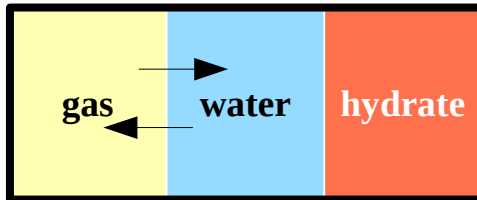
- Fully implicit cell centered finite volume method based discretization  
two-point finite difference flux approximation  
fully upwinded convective fluxes
- Nonlinear **Complementary Constraints** for vanishing gas phase, [Lauser,2011]
- **Semismooth Newton**'s method for Linearization,  
**Active-sets strategy**
- **SuperLU** Linear Solver

Implementation in **DUNE-PDElab** framework  
[Bastian2010]  
(<http://www.dune-project.org>)

$$S_\alpha - \max \left\{ 0, S_\alpha - \left( 1 - \sum_{\kappa} \chi_\alpha^\kappa \right) \right\} = 0, \quad \forall \alpha.$$

Equivalent form of the NCP  
non-differentiable,  
but semi-smooth

# Mathematical Model



**NUMERICAL SOLUTION**

- Fully implicit cell centered finite volume method based discretization  
two-point finite difference flux approximation  
fully upwinded convective fluxes
- Nonlinear **Complementary Constraints** for vanishing gas phase, [Lauser,2011]
- **Semismooth Newton**'s method for Linearization,  
**Active-sets strategy**
- **SuperLU** Linear Solver

Implementation in **DUNE-PDElab** framework  
[Bastian2010]  
(<http://www.dune-project.org>)

$$S_\alpha - \max \left\{ 0, S_\alpha - \left( 1 - \sum_{\kappa} \chi_{\alpha}^{\kappa} \right) \right\} = 0, \quad \forall \alpha.$$

$$\mathcal{A}_\alpha := \left\{ j \in \mathcal{N} : (S_\alpha)_j - \left( 1 - \sum_{\kappa} (\chi_{\alpha}^{\kappa})_j \right) > 0 \right\}$$

$$\mathcal{I}_\alpha := \mathcal{N} \setminus \mathcal{A}_\alpha$$

# Field-scale Example

## BCL System in Danube Paleo Delta

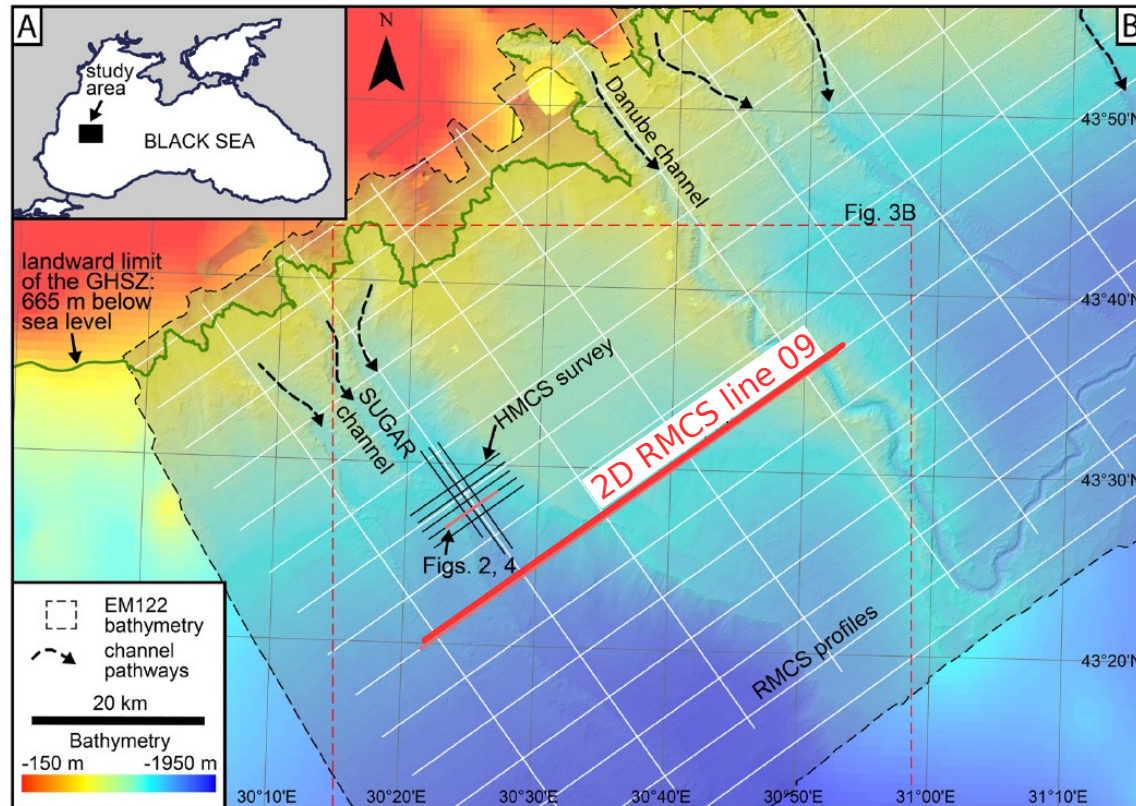


Fig.: Overview map of 2D high-resolution multichannel seismic (HMCS) survey, and 2D regional multichannel seismic (RMCS) survey.

Bathymetry and seismic data were acquired during **R/V Maria S. Merian** cruise **MSM34** in 2013–2014.

# Field-scale Example

## BCL System in Danube Paleo Delta

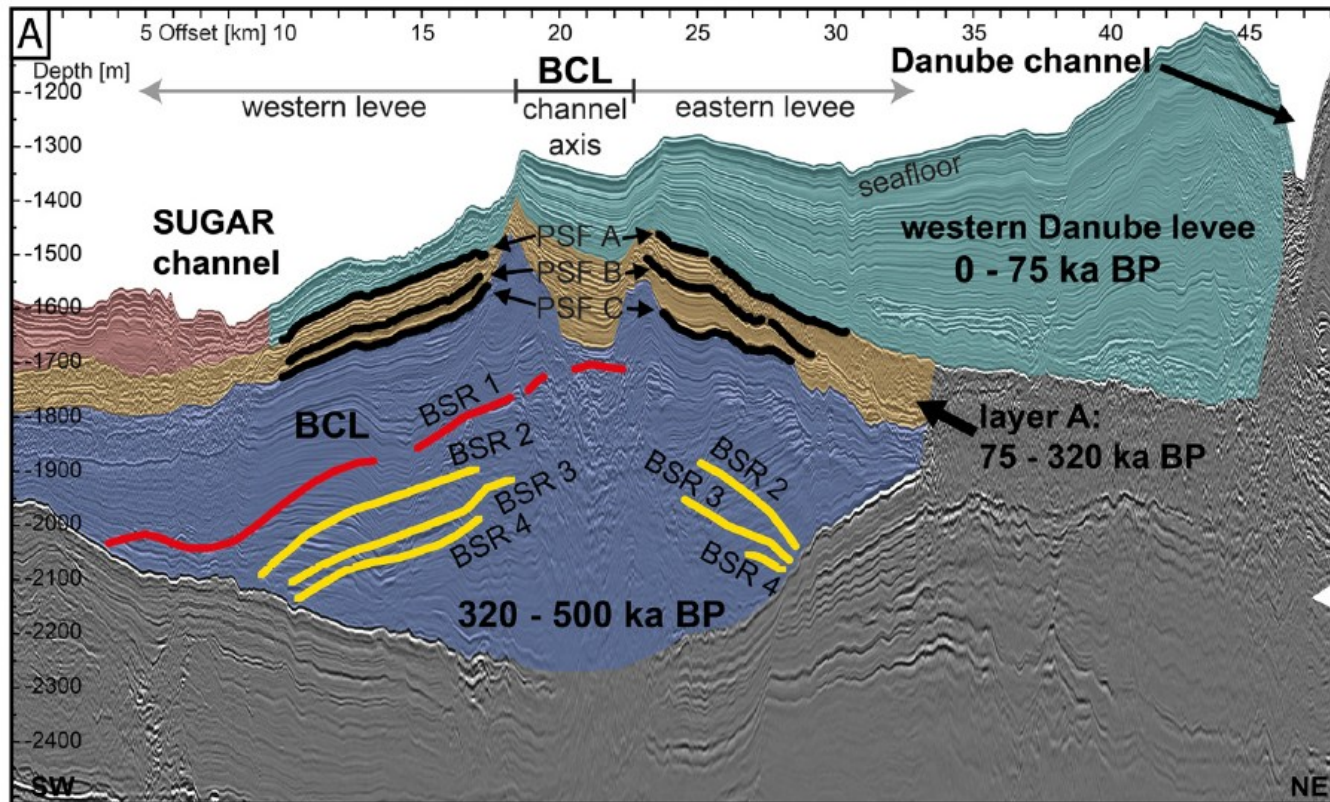


Fig.: 2D RMCS line 09  
Interpretation of the seismic data [Zander2017]



# Field-scale Example BCL System in Danube Paleo Delta

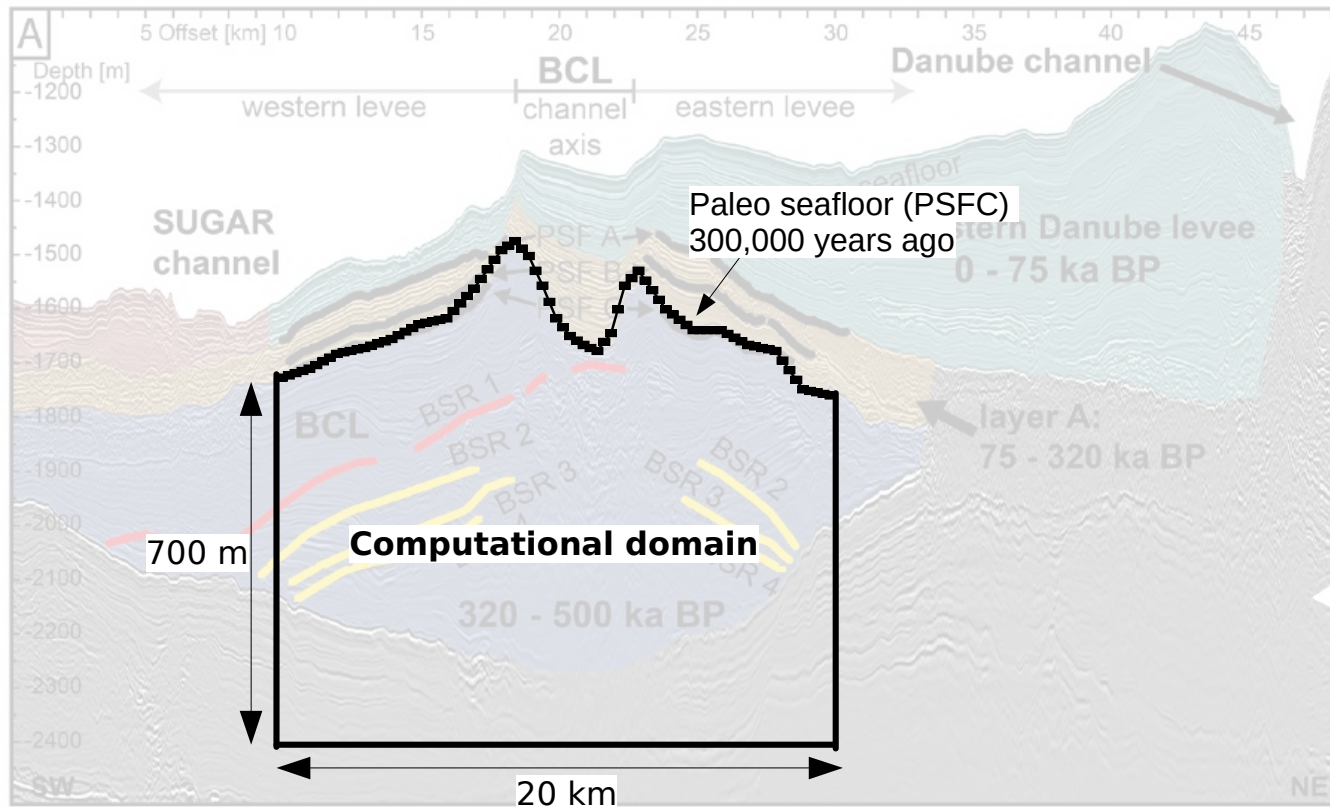
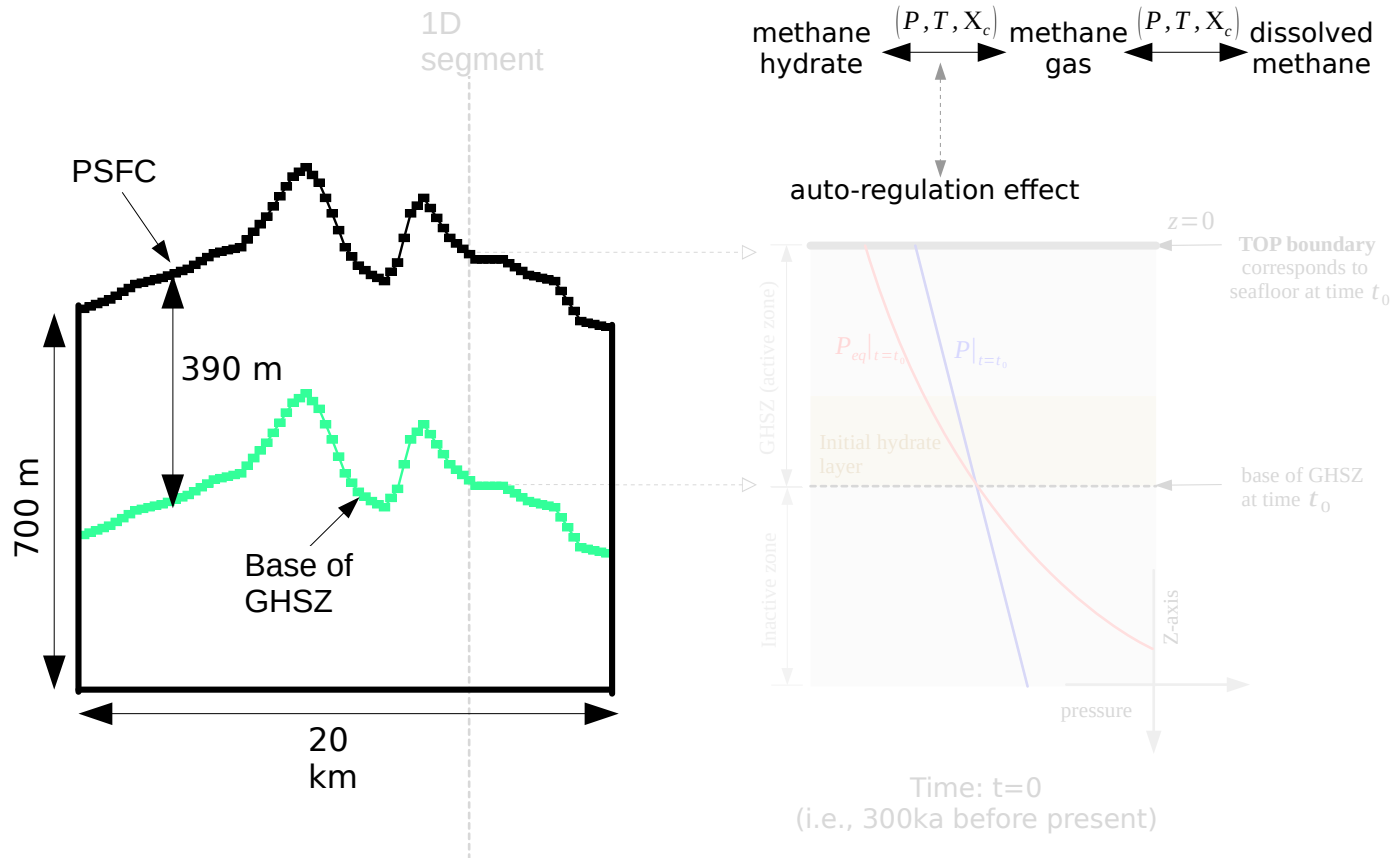


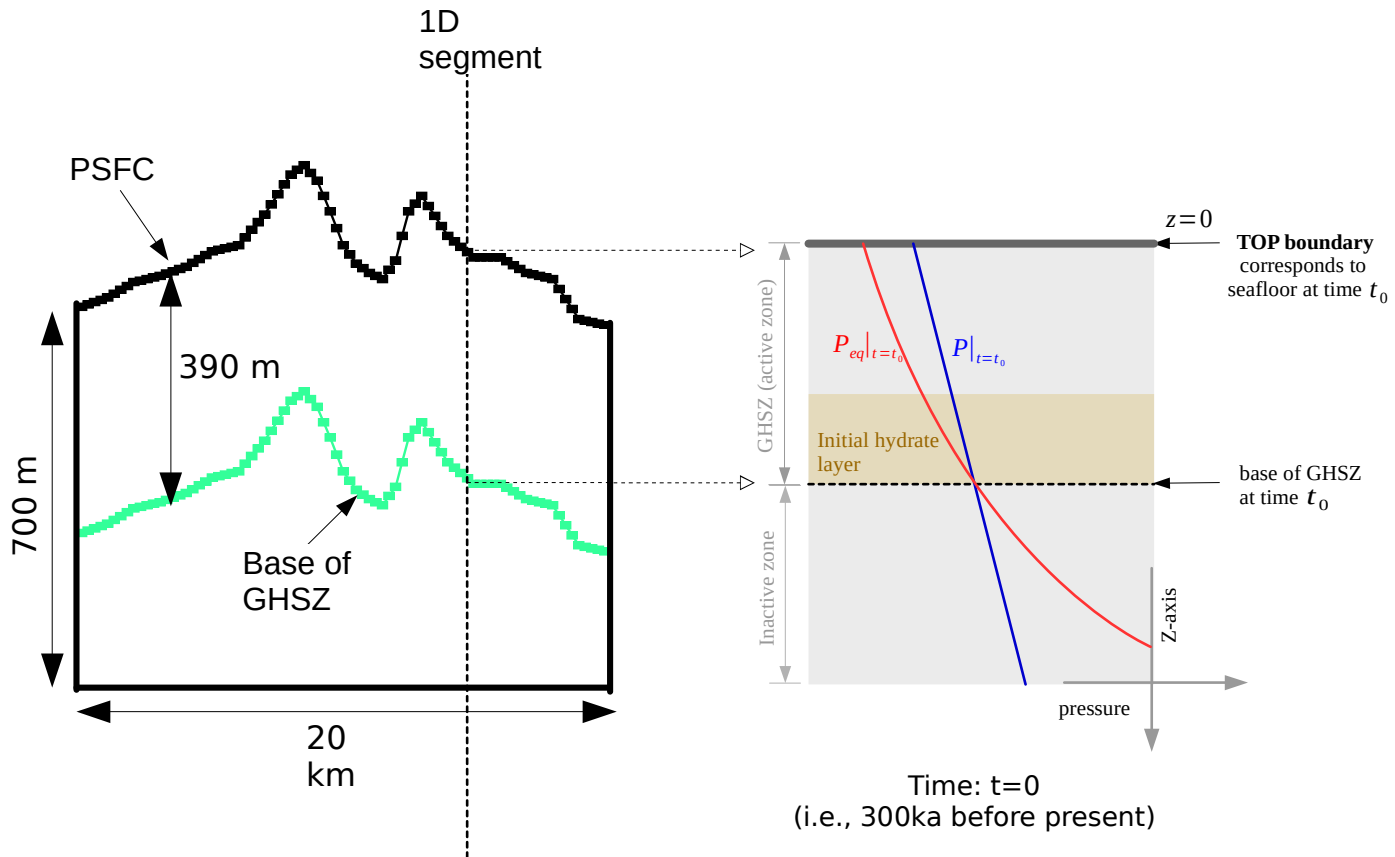
Fig.: 2D RMCS line 09  
Interpretation of the seismic data [Zander2017]

# Field-scale Example

## BCL System in Danube Paleo Delta

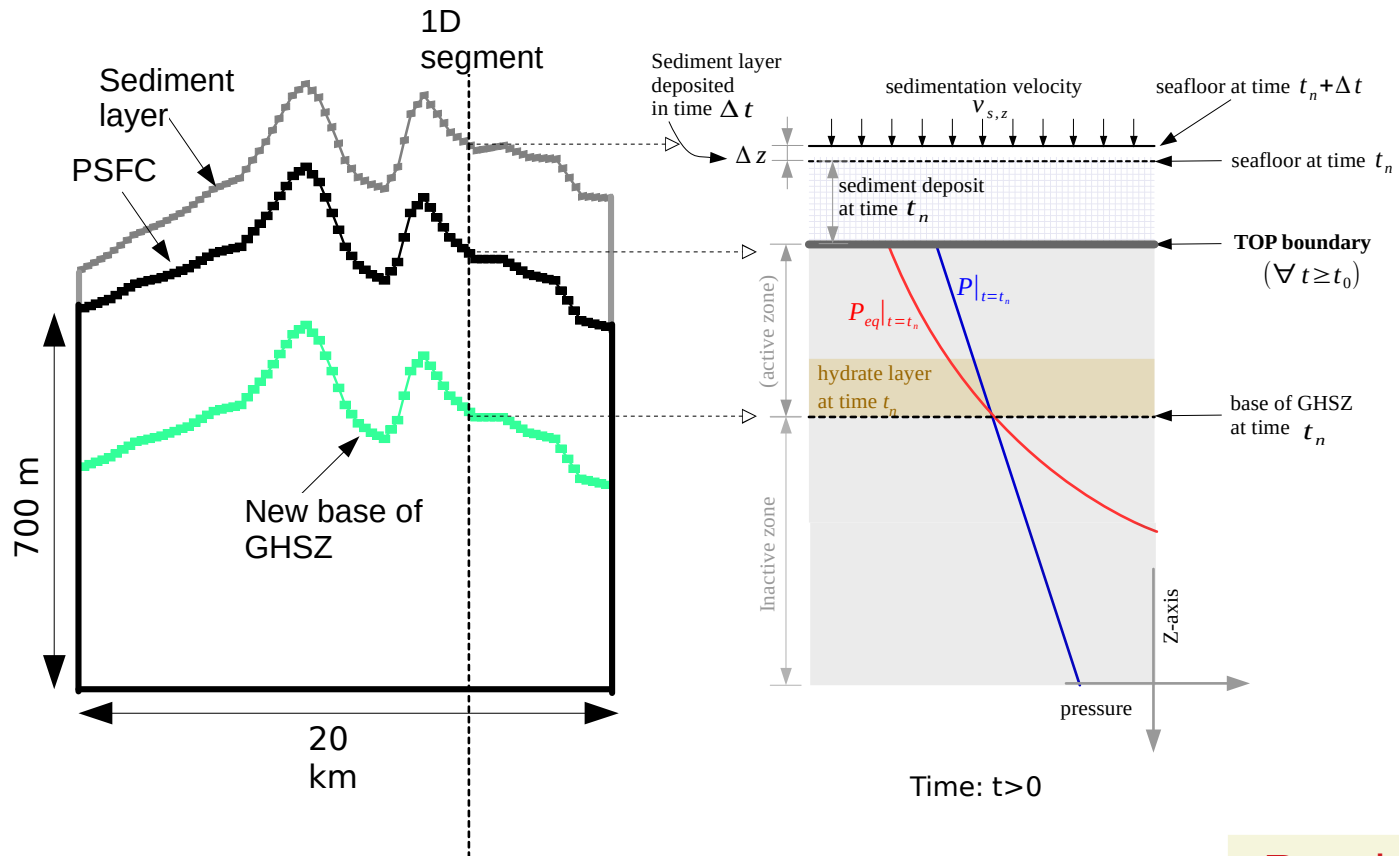


# Field-scale Example BCL System in Danube Paleo Delta



# Field-scale Example

## BCL System in Danube Paleo Delta

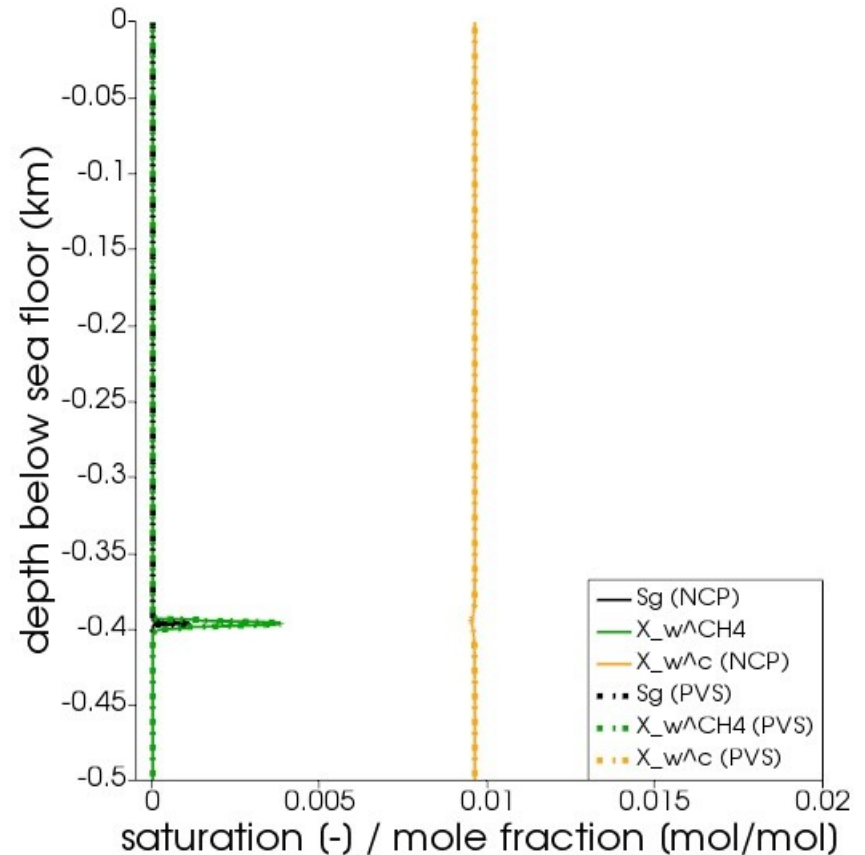
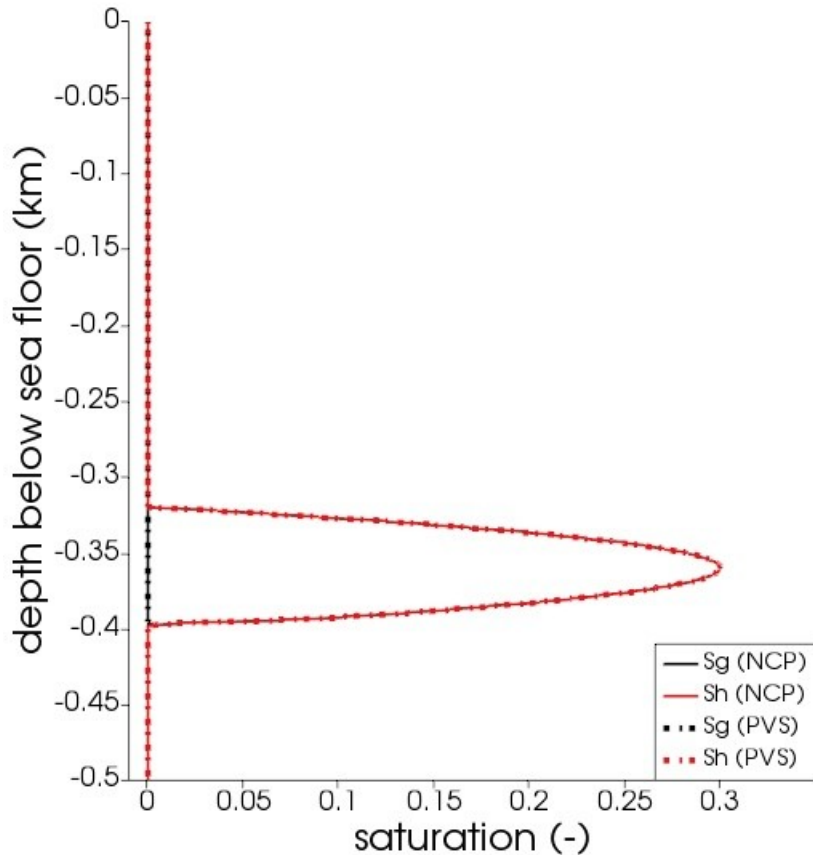


Results

# Field-scale Example

## BCL System in Danube Paleo Delta

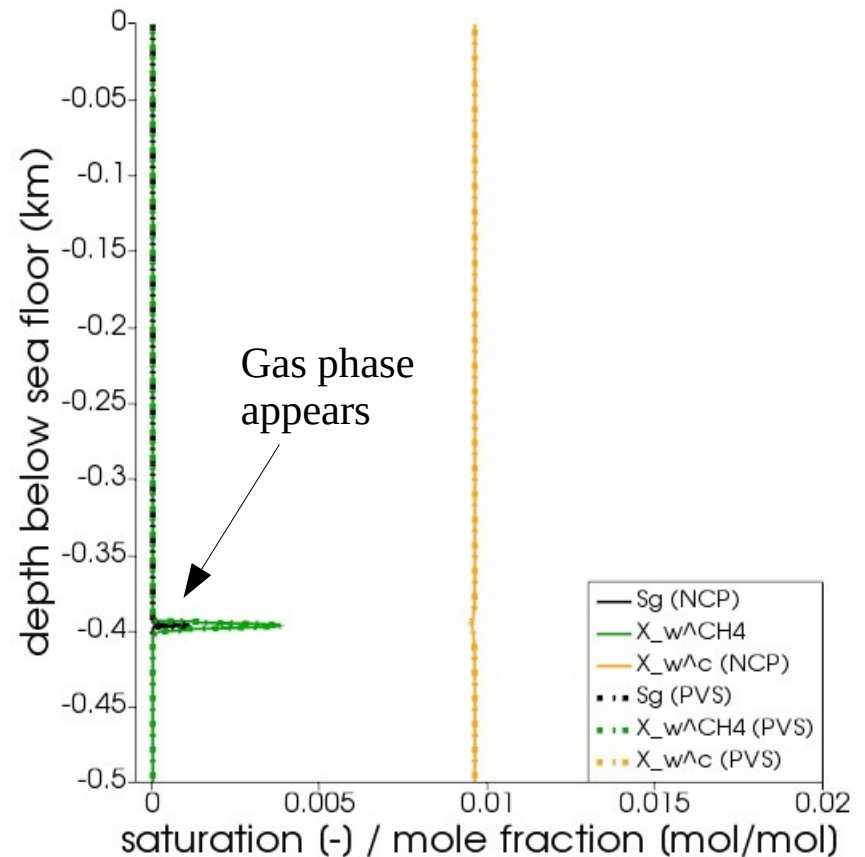
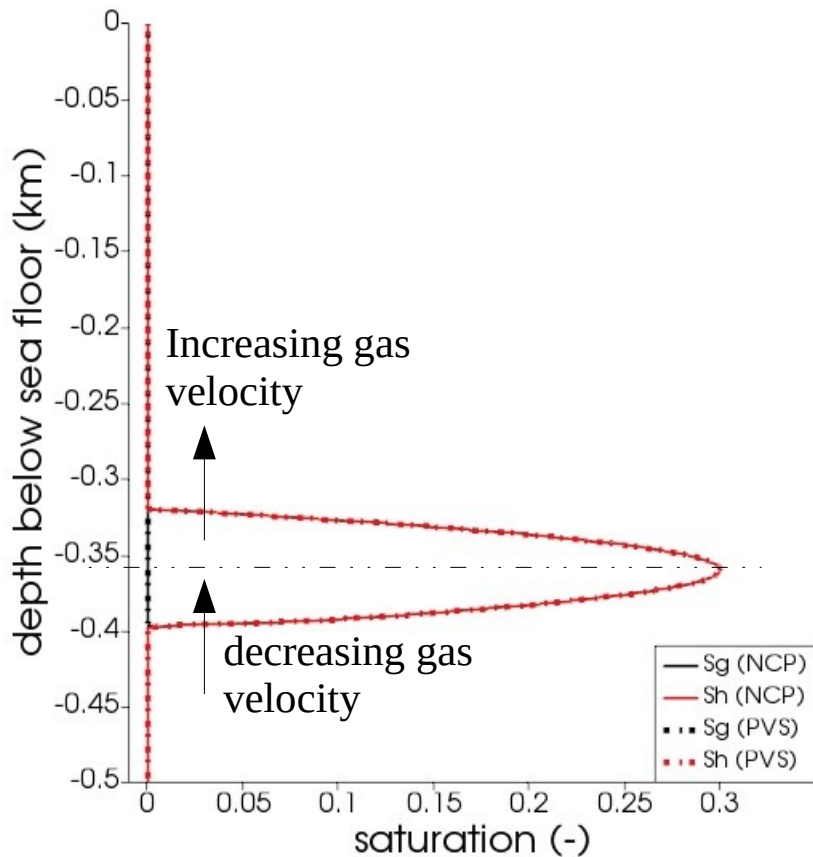
Time = 19,500 years



# Field-scale Example

## BCL System in Danube Paleo Delta

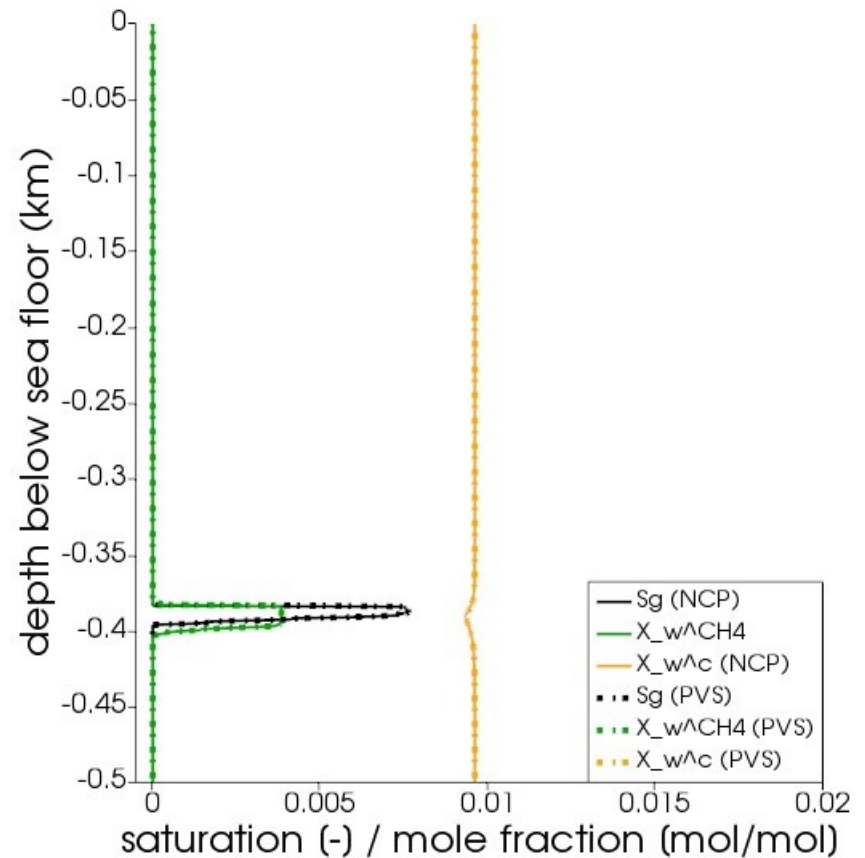
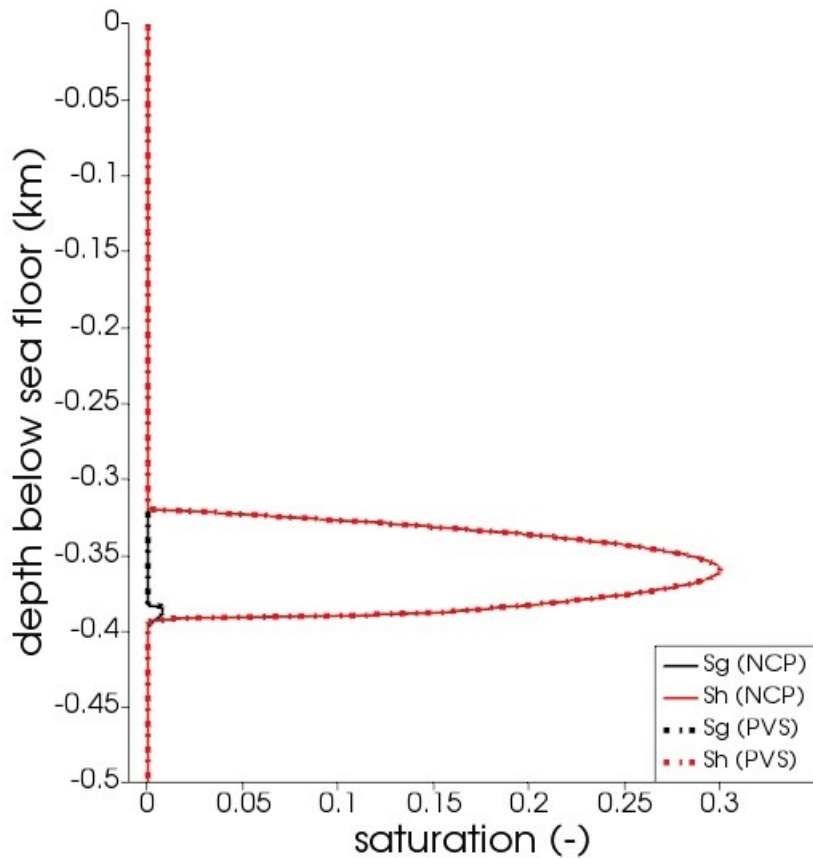
Time = 19,500 years



# Field-scale Example

## BCL System in Danube Paleo Delta

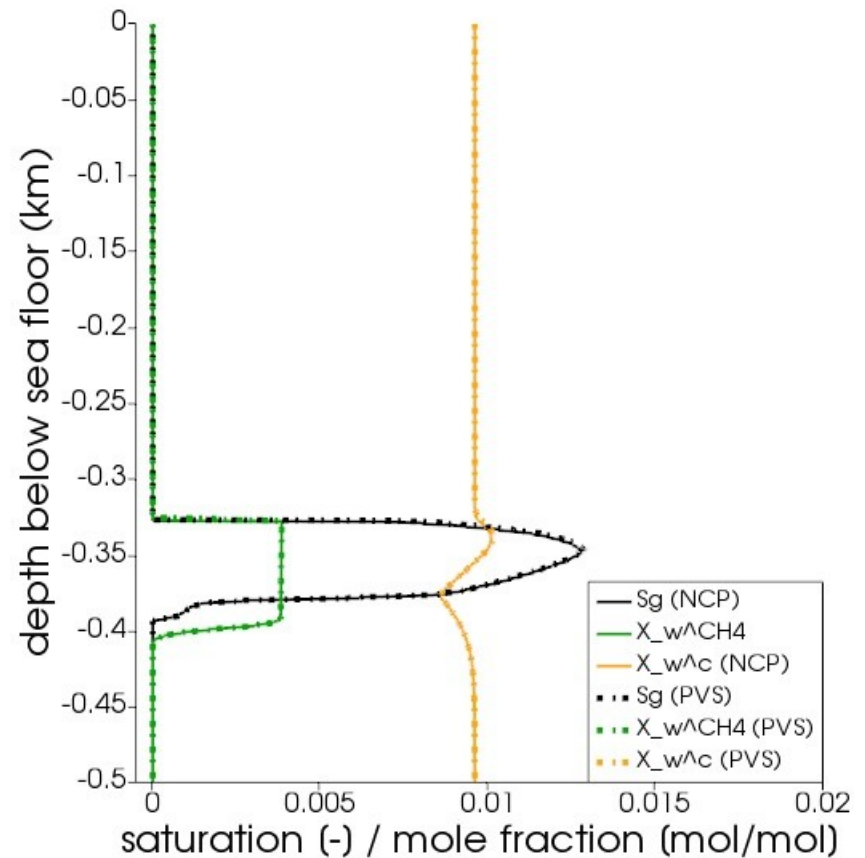
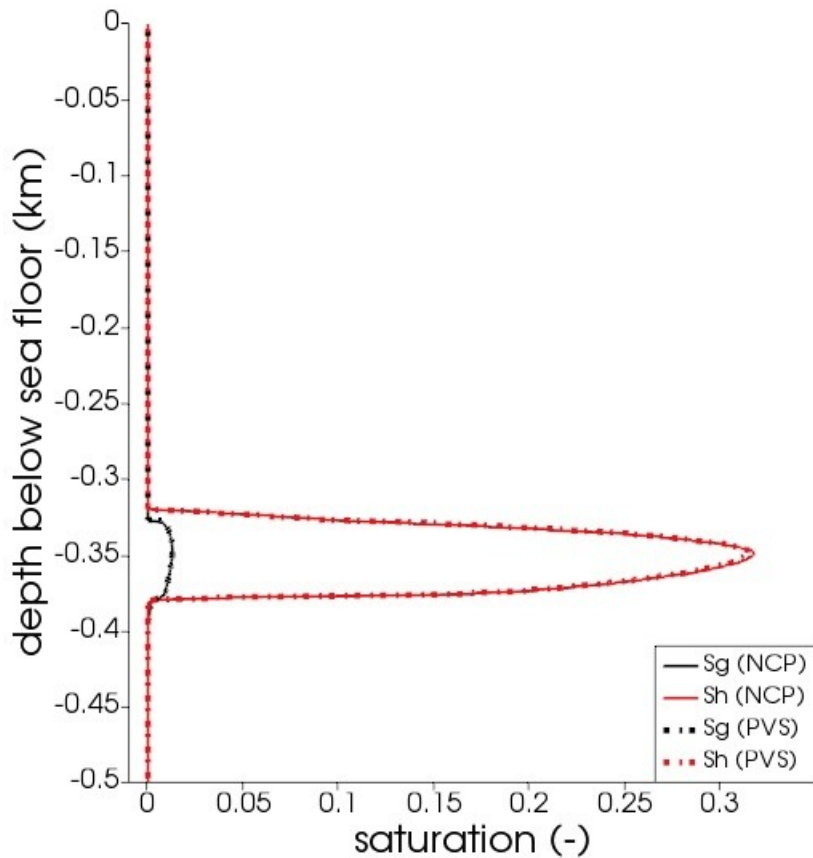
Time = 30,000 years



# Field-scale Example

## BCL System in Danube Paleo Delta

Time = 60,000 years

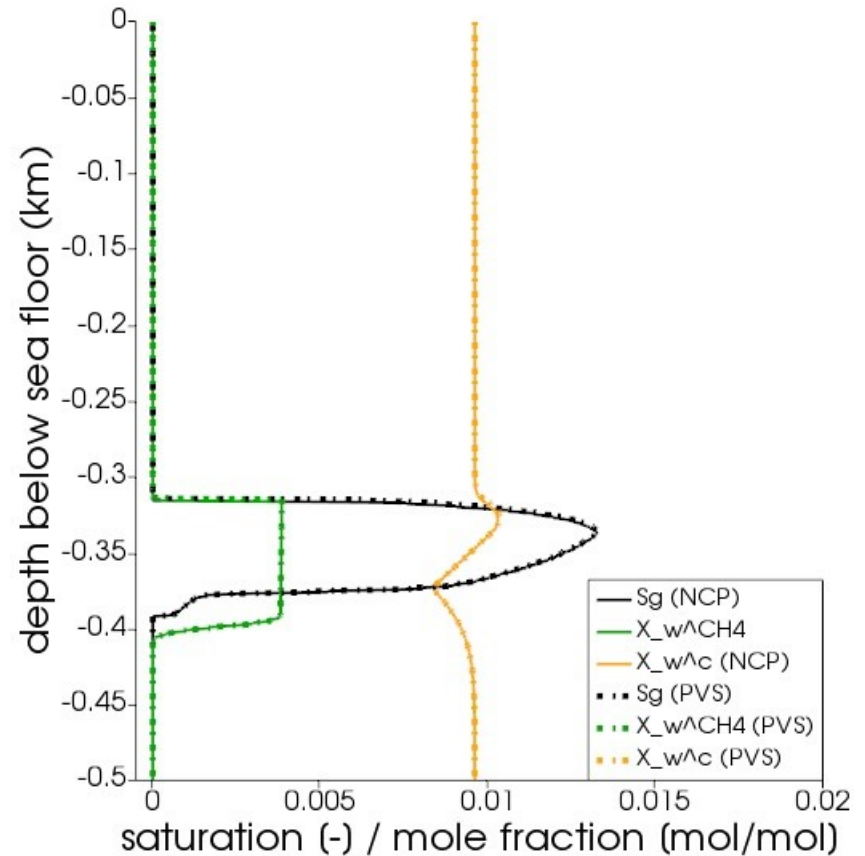
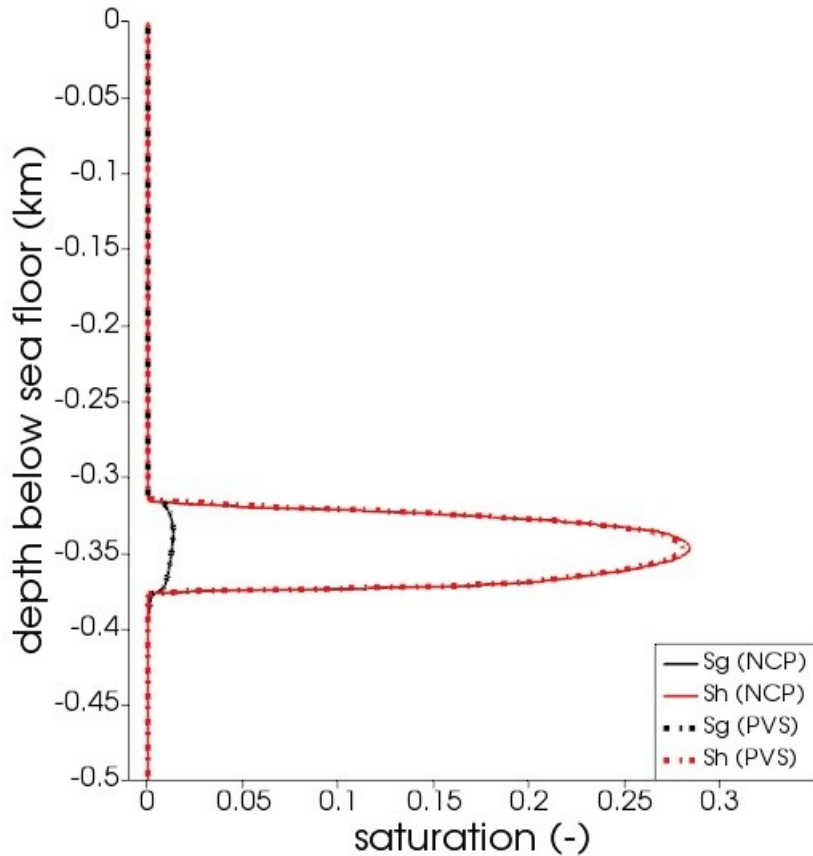




# Field-scale Example

## BCL System in Danube Paleo Delta

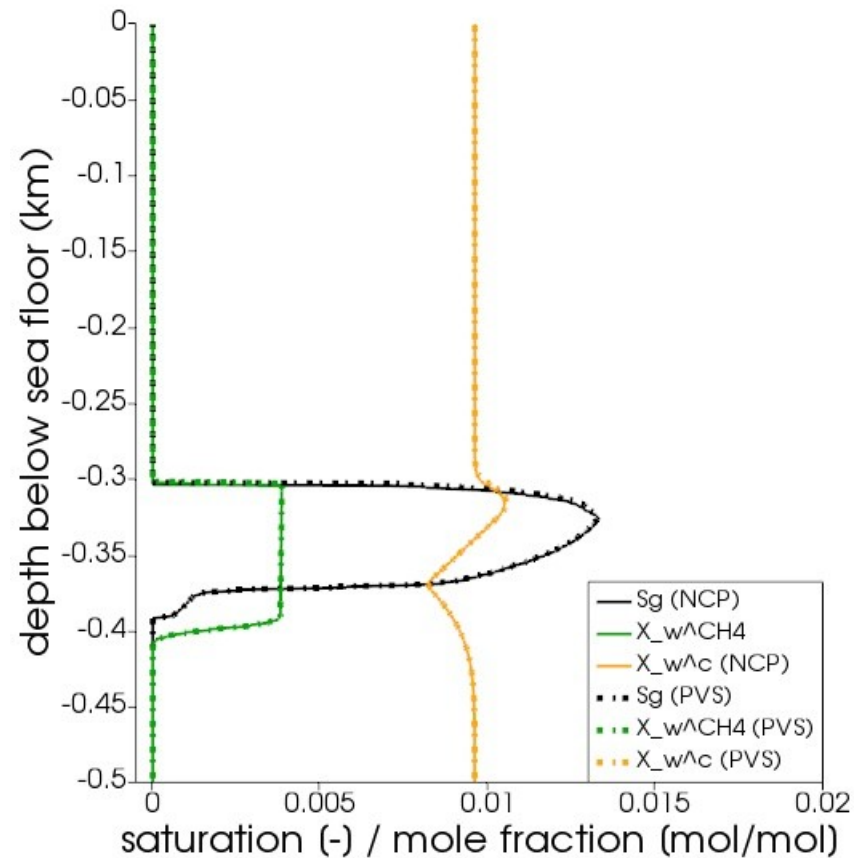
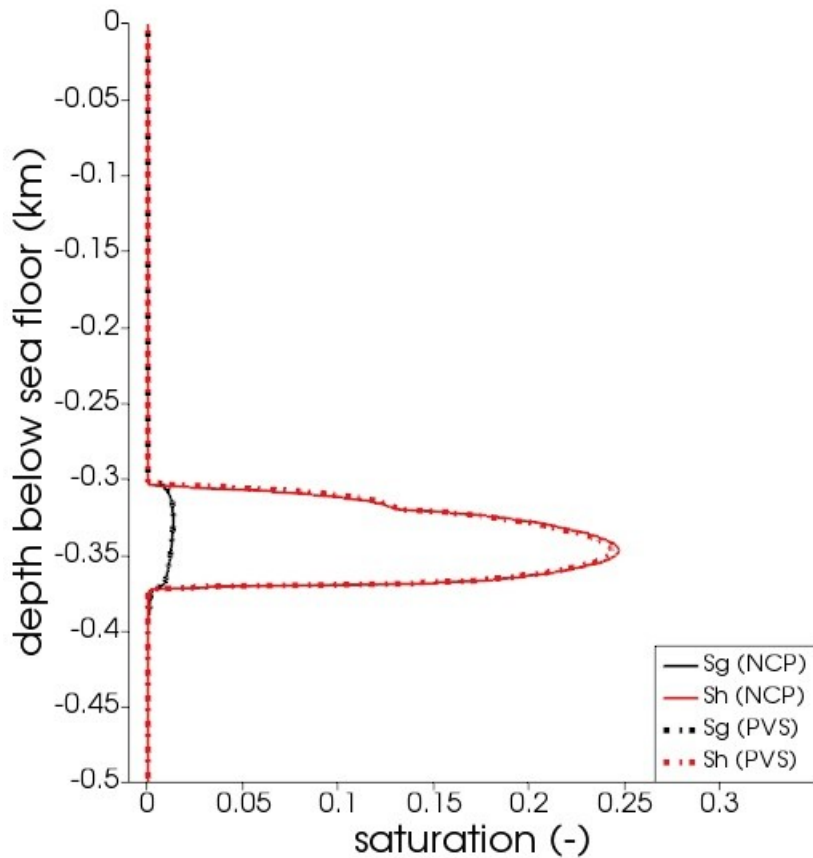
Time = 67,500 years



# Field-scale Example

## BCL System in Danube Paleo Delta

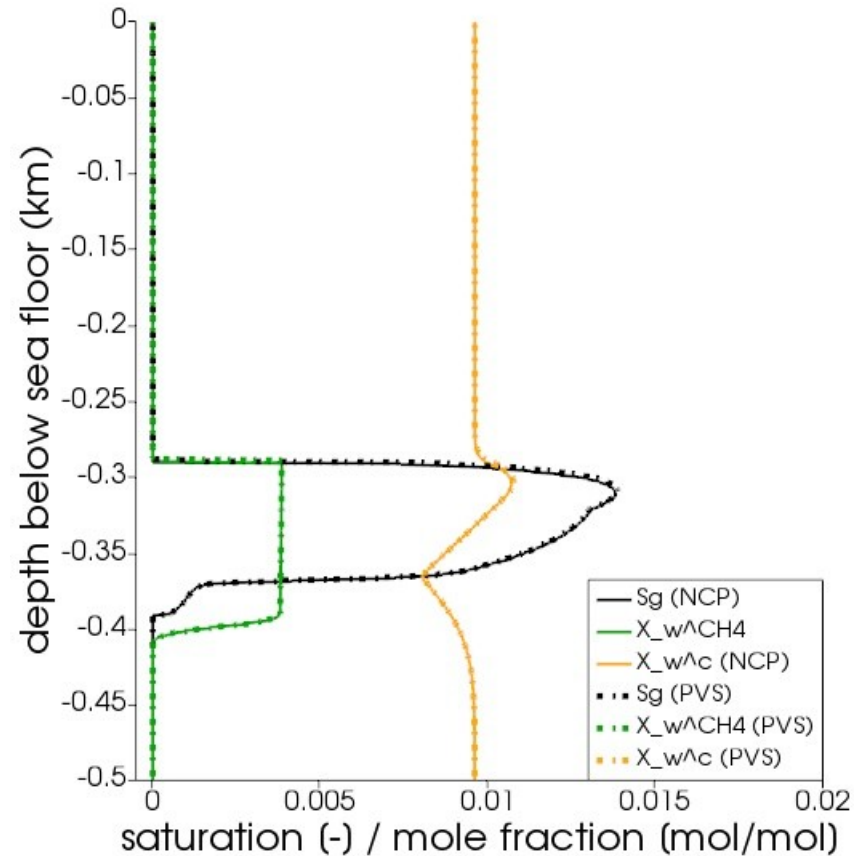
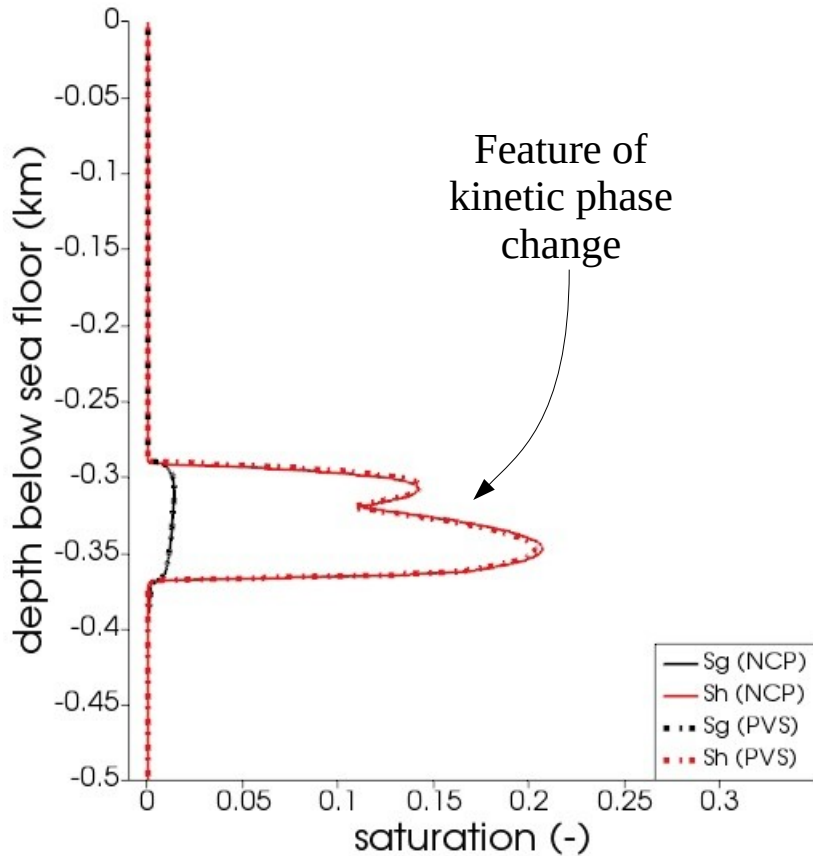
Time = 75,000 years



# Field-scale Example

## BCL System in Danube Paleo Delta

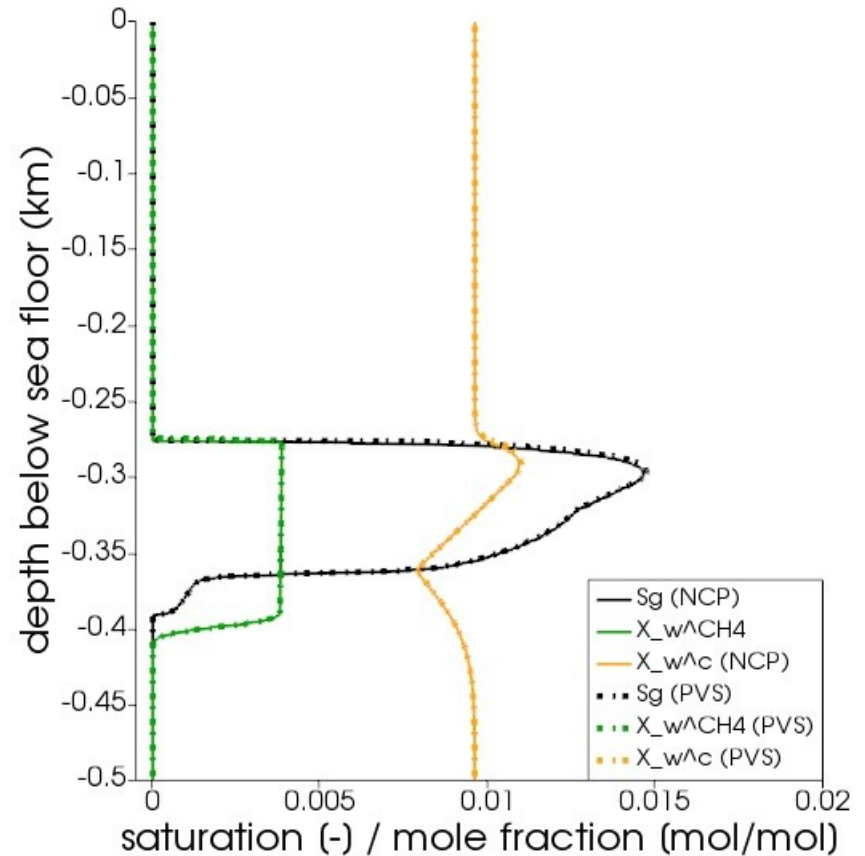
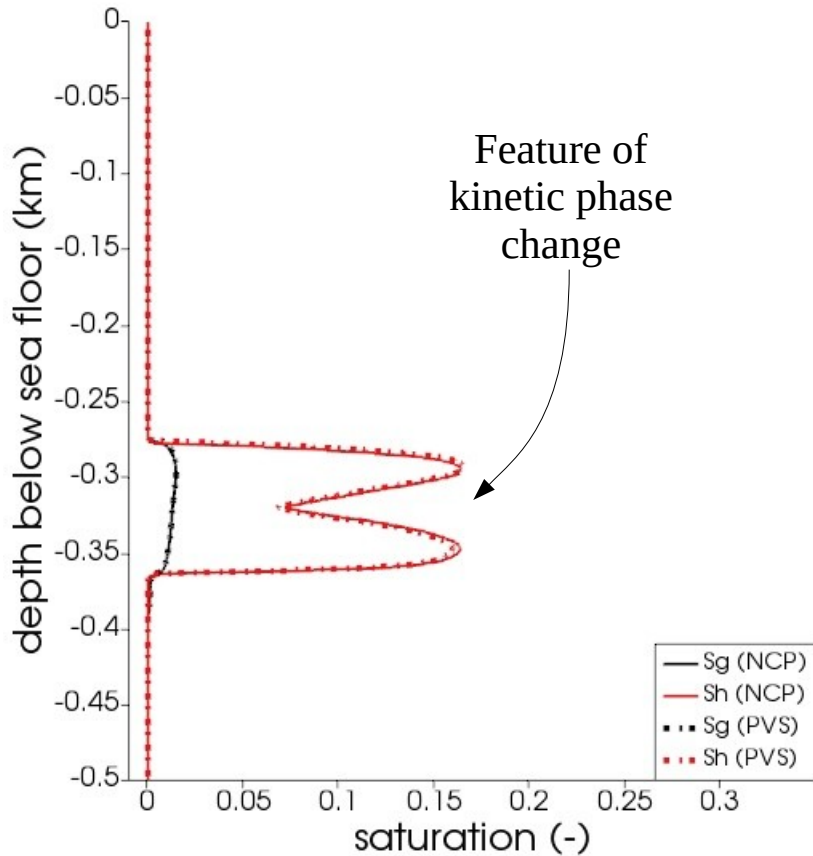
Time = 82,500 years



# Field-scale Example

## BCL System in Danube Paleo Delta

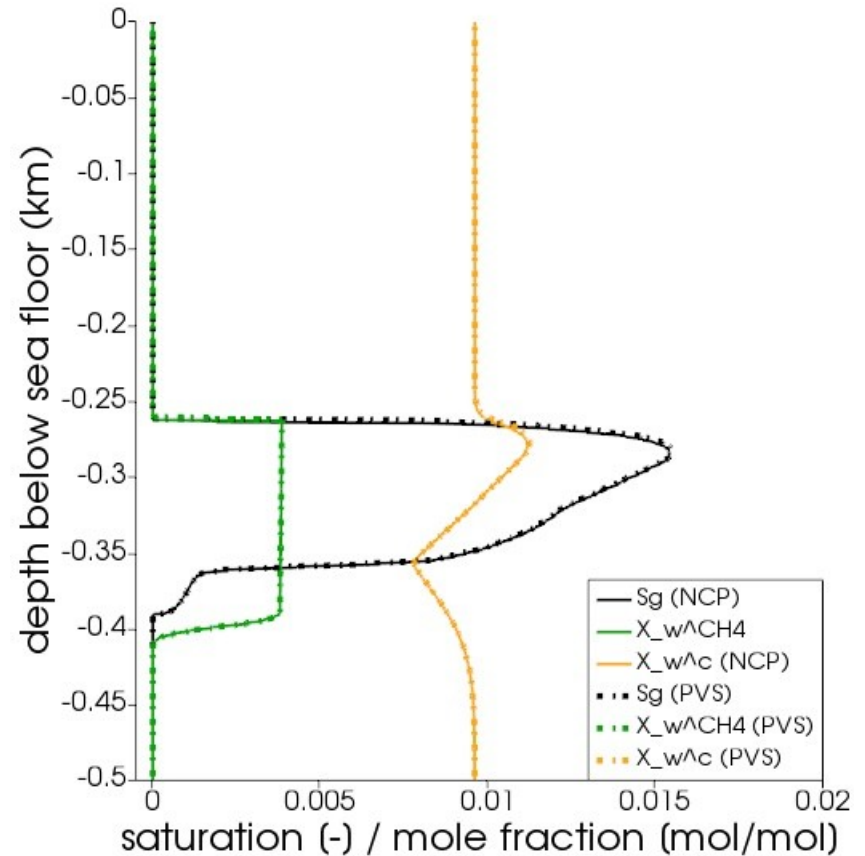
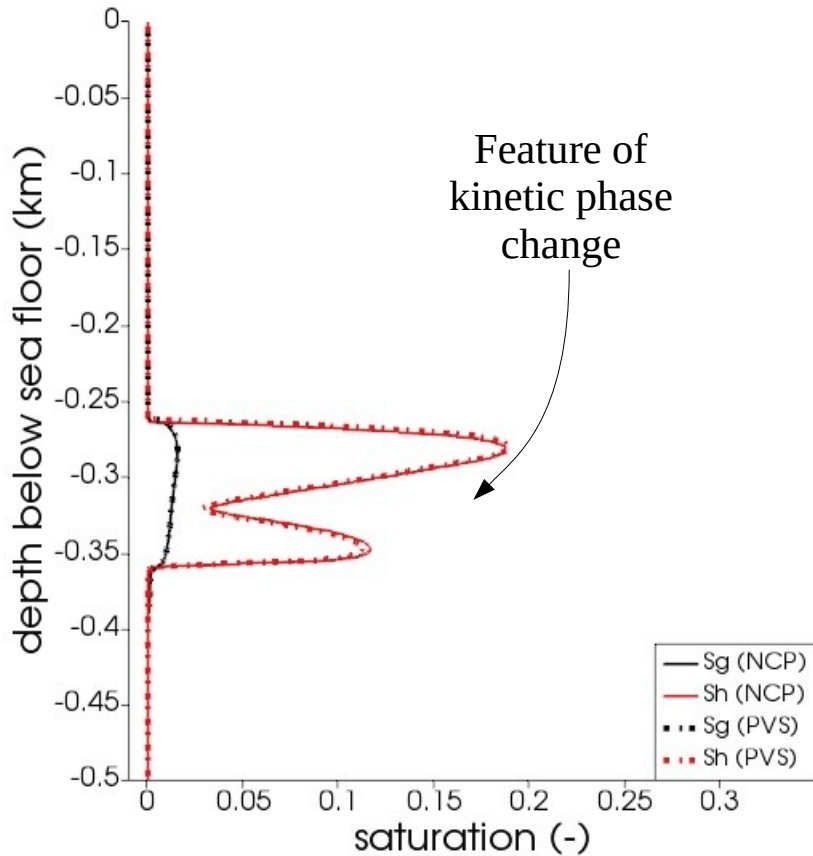
Time = 90,000 years



# Field-scale Example

## BCL System in Danube Paleo Delta

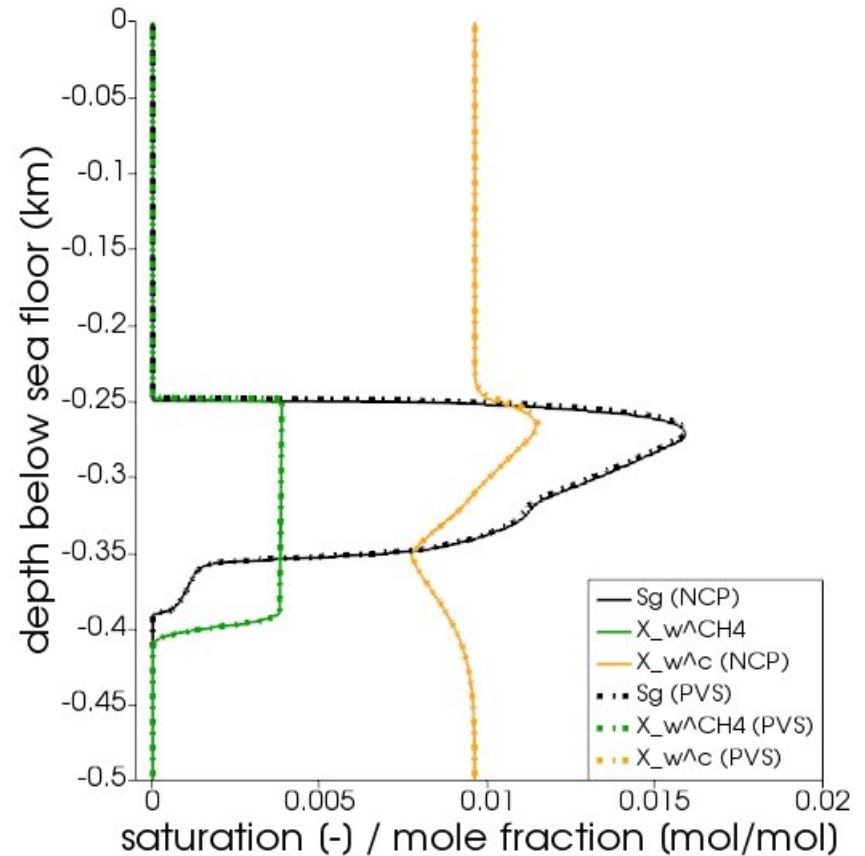
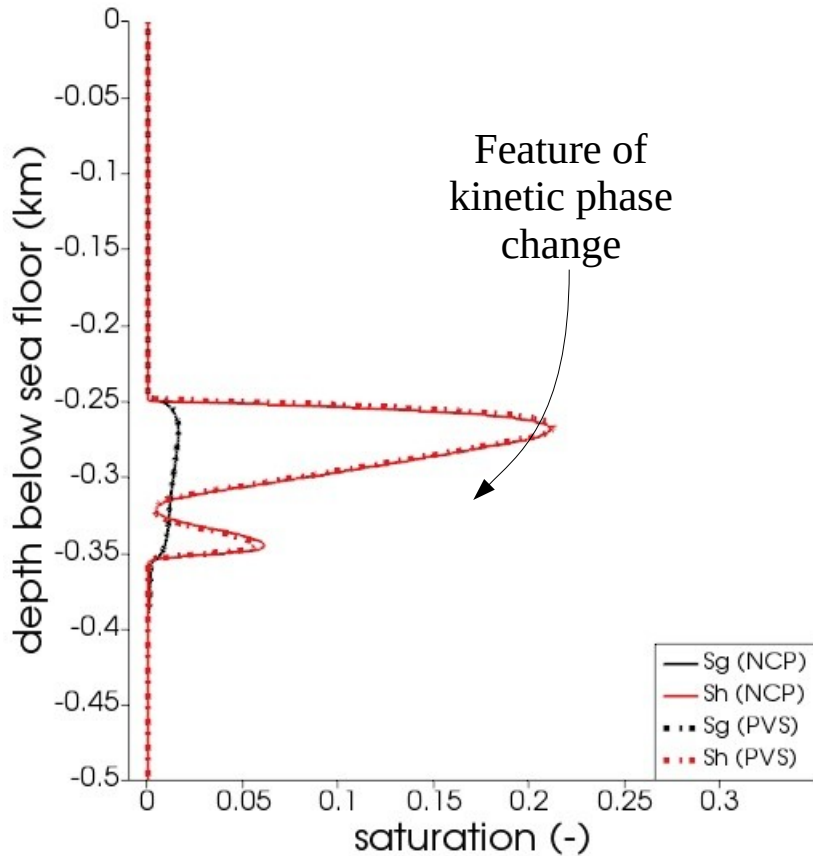
Time = 97,500 years



# Field-scale Example

## BCL System in Danube Paleo Delta

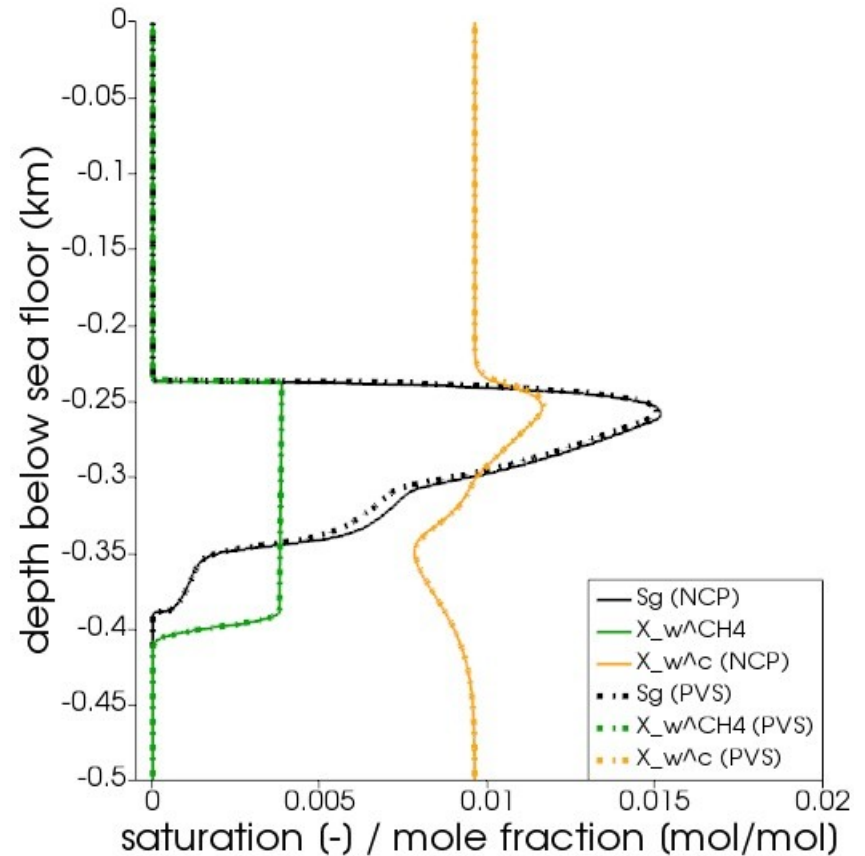
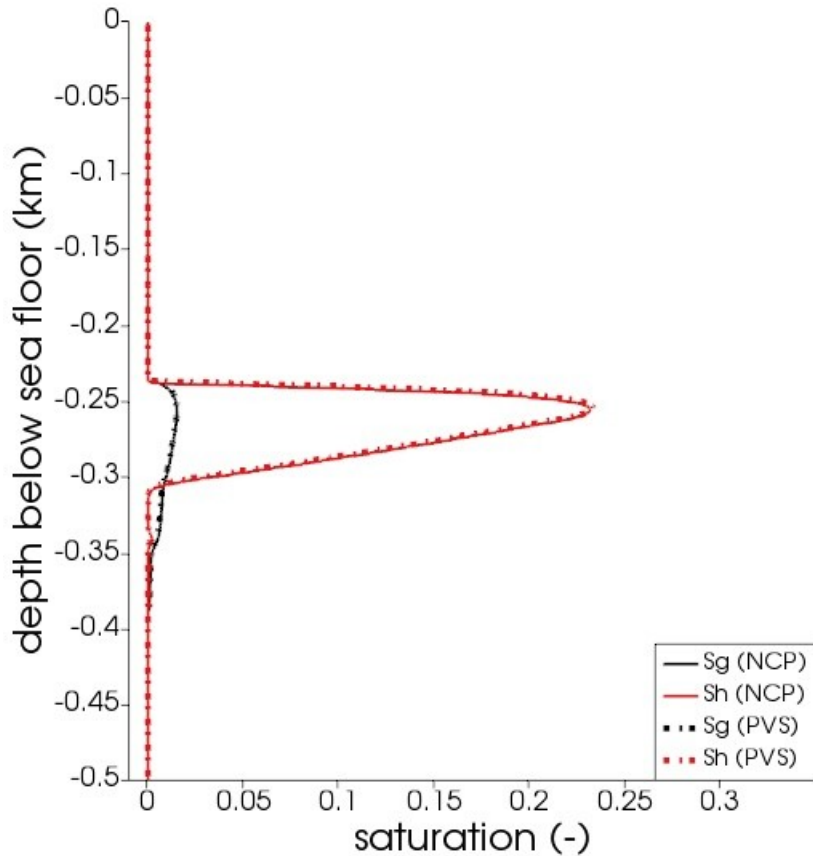
Time = 105,000 years



# Field-scale Example

## BCL System in Danube Paleo Delta

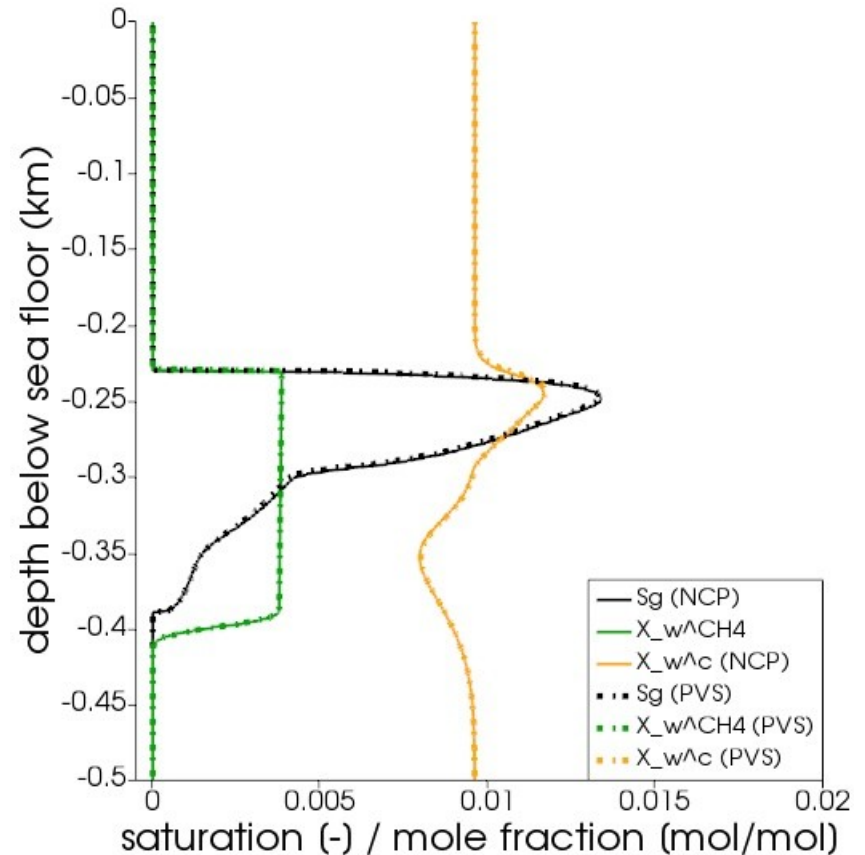
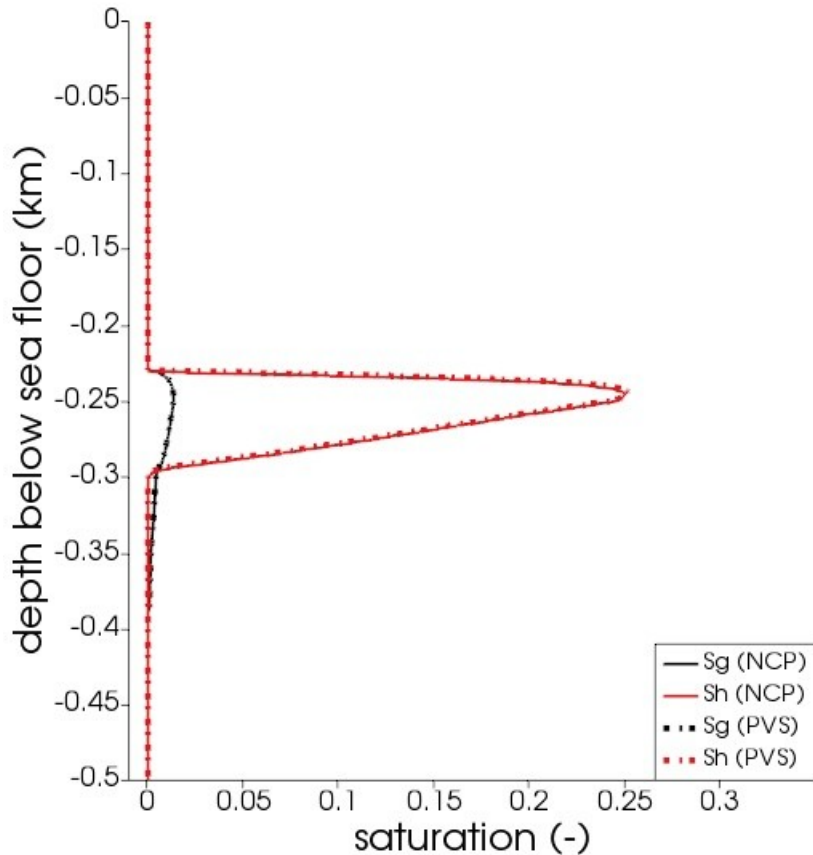
Time = 112,500 years



# Field-scale Example

## BCL System in Danube Paleo Delta

Time = 120,000 years

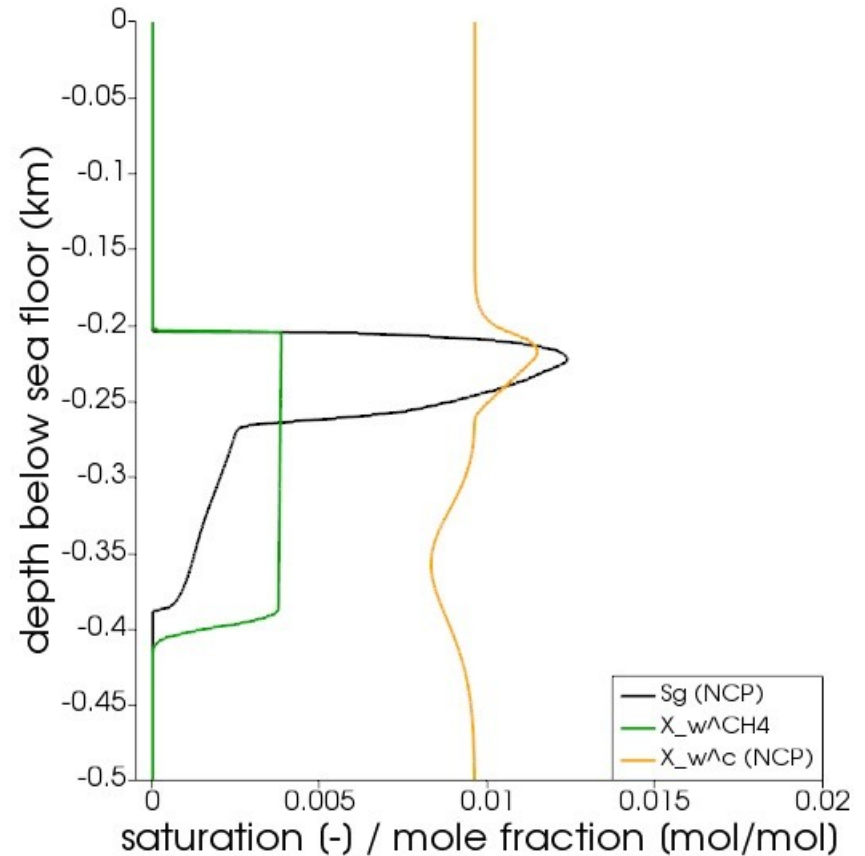
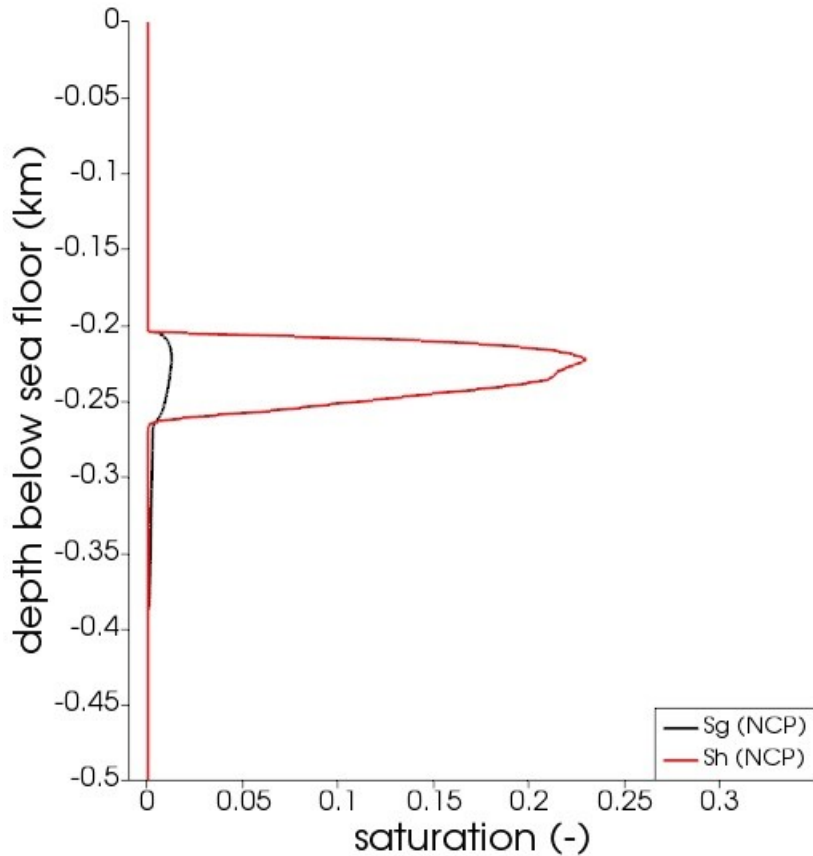




# Field-scale Example

## BCL System in Danube Paleo Delta

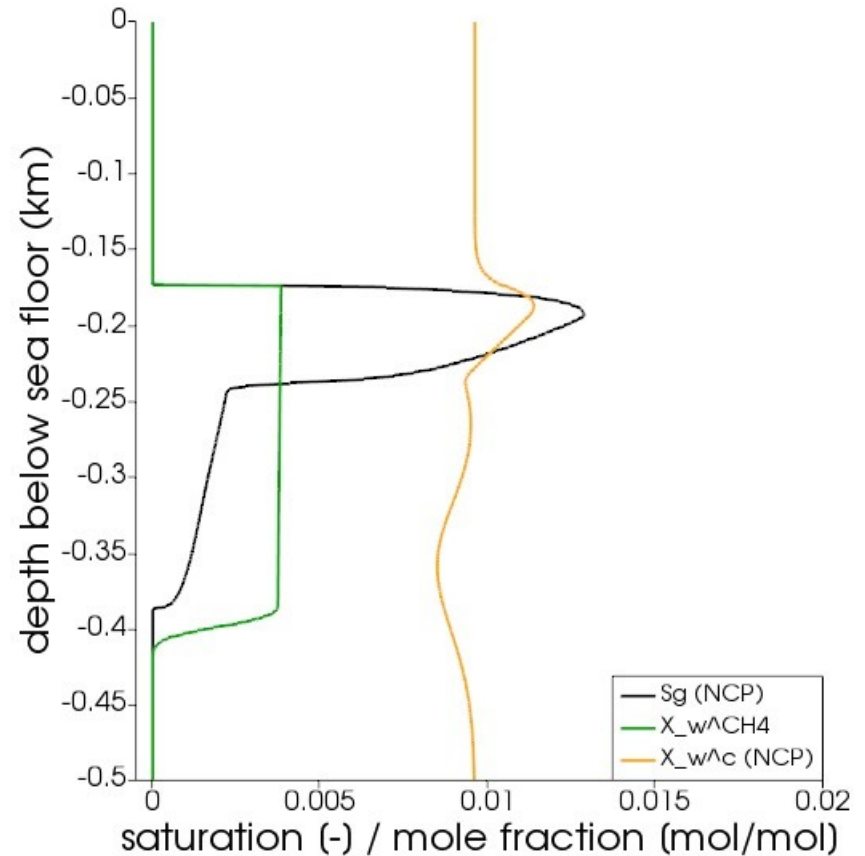
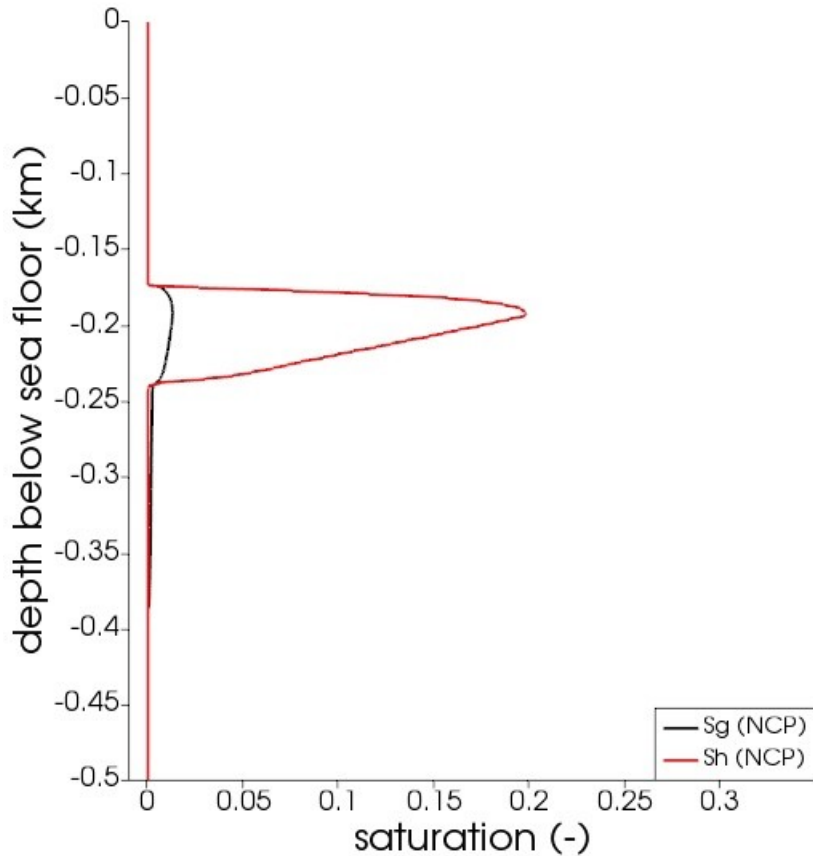
Time = 150,000 years



# Field-scale Example

## BCL System in Danube Paleo Delta

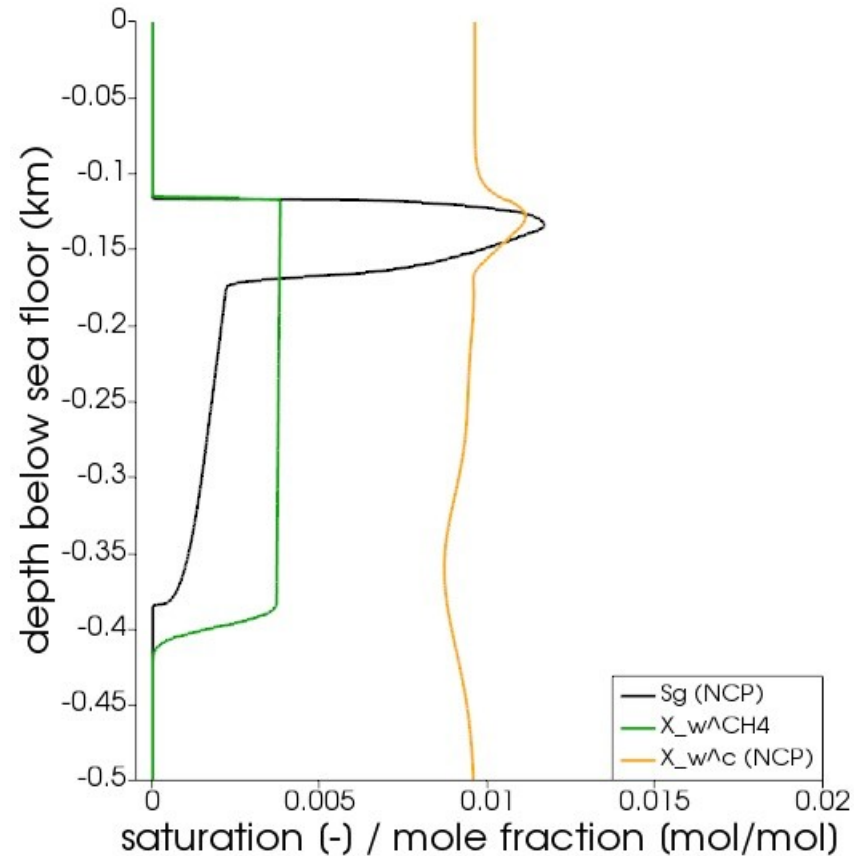
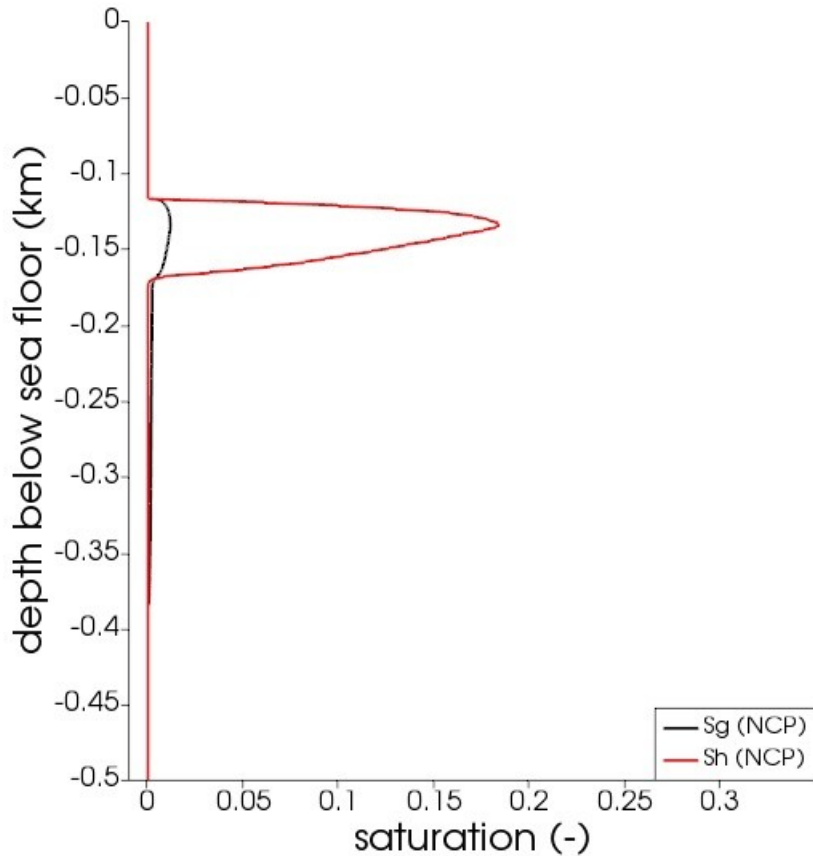
Time = 180,000 years



# Field-scale Example

## BCL System in Danube Paleo Delta

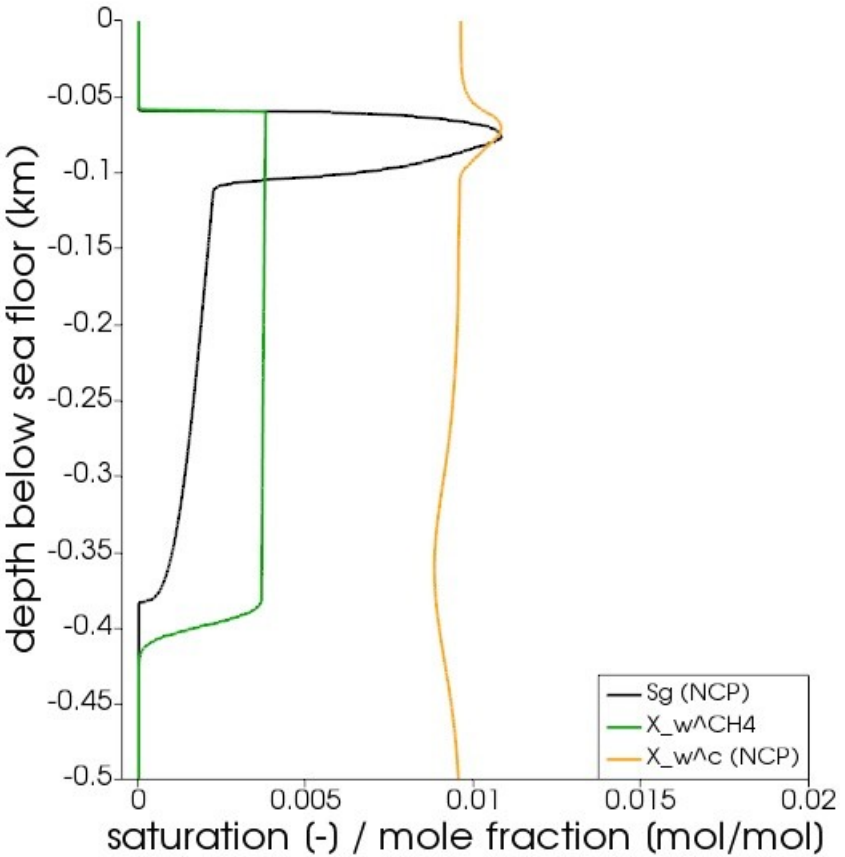
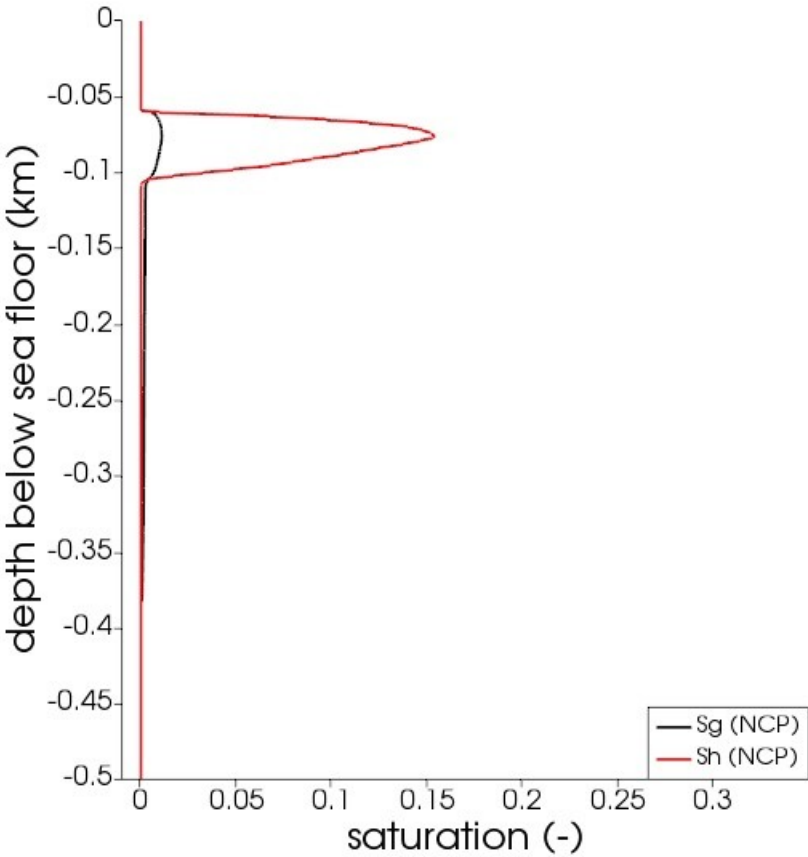
Time = 240,000 years



# Field-scale Example

## BCL System in Danube Paleo Delta

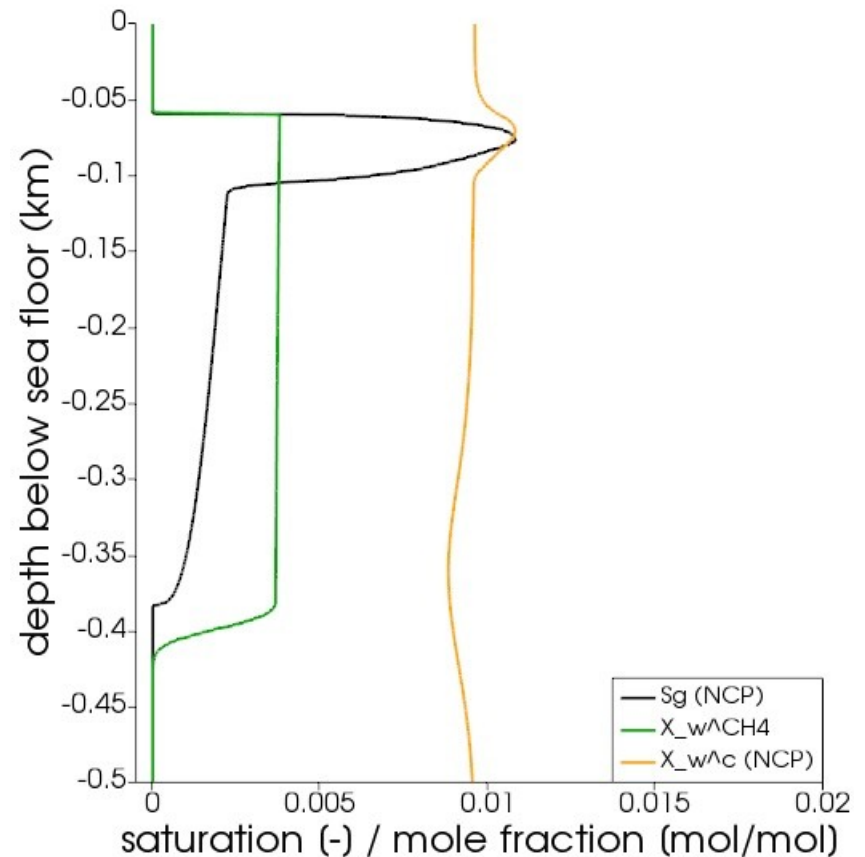
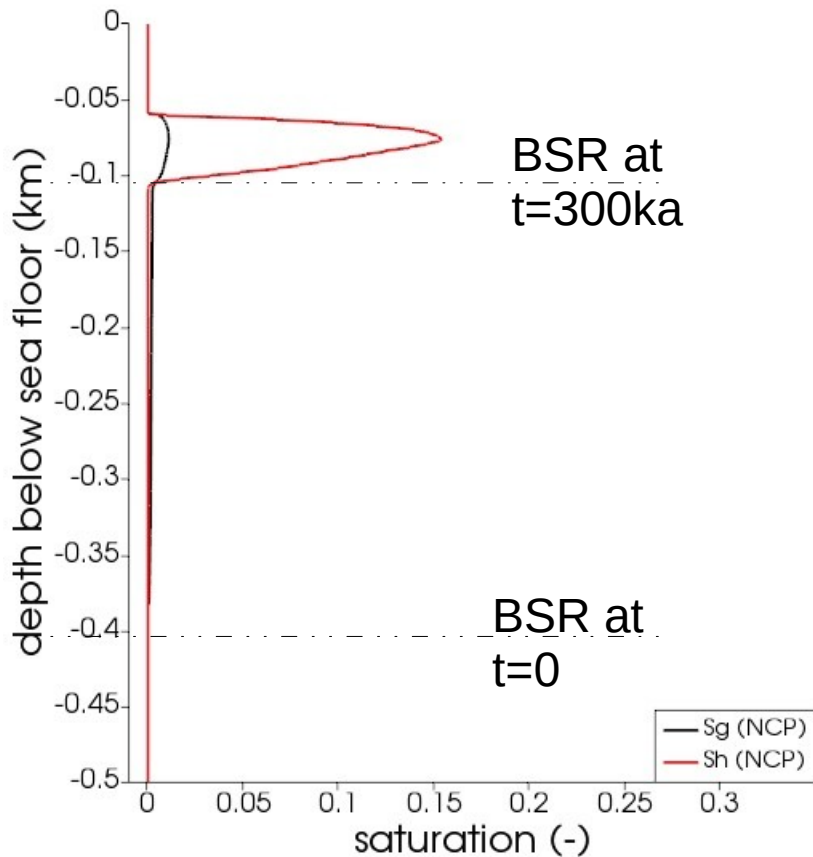
Time = 300,000 years



# Field-scale Example

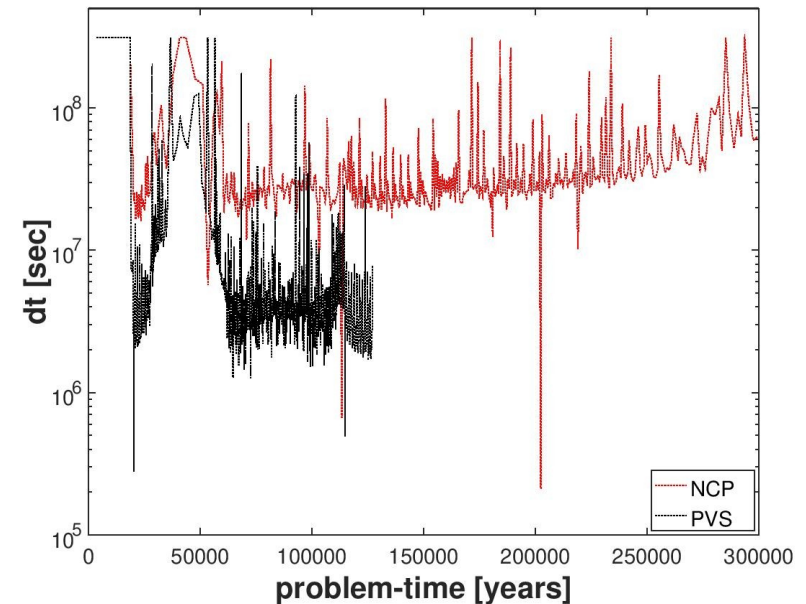
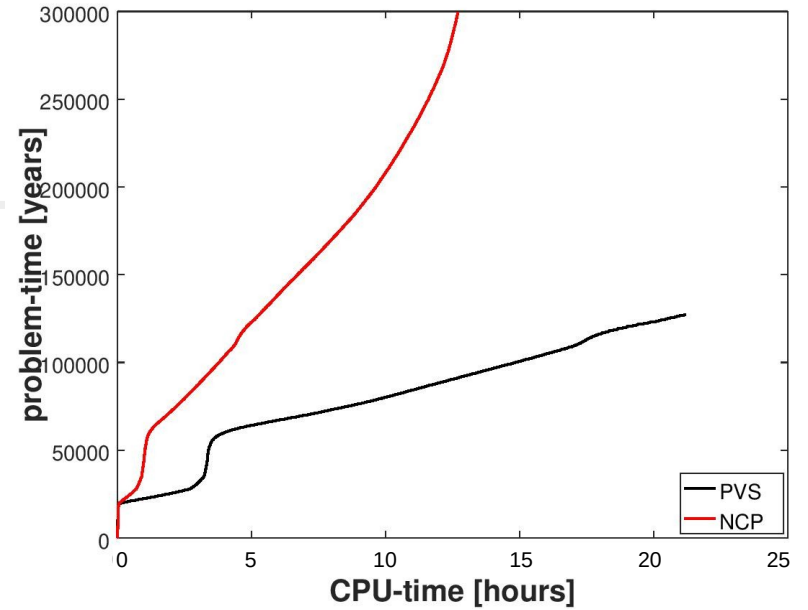
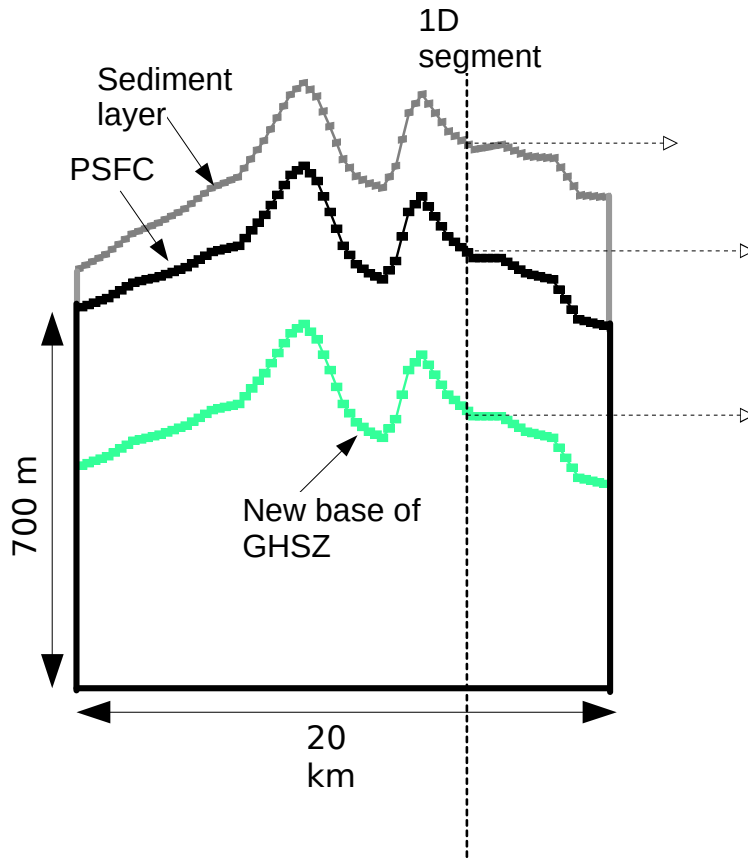
## BCL System in Danube Paleo Delta

Time = 300,000 years



# Field-scale Example

## BCL System in Danube Paleo Delta

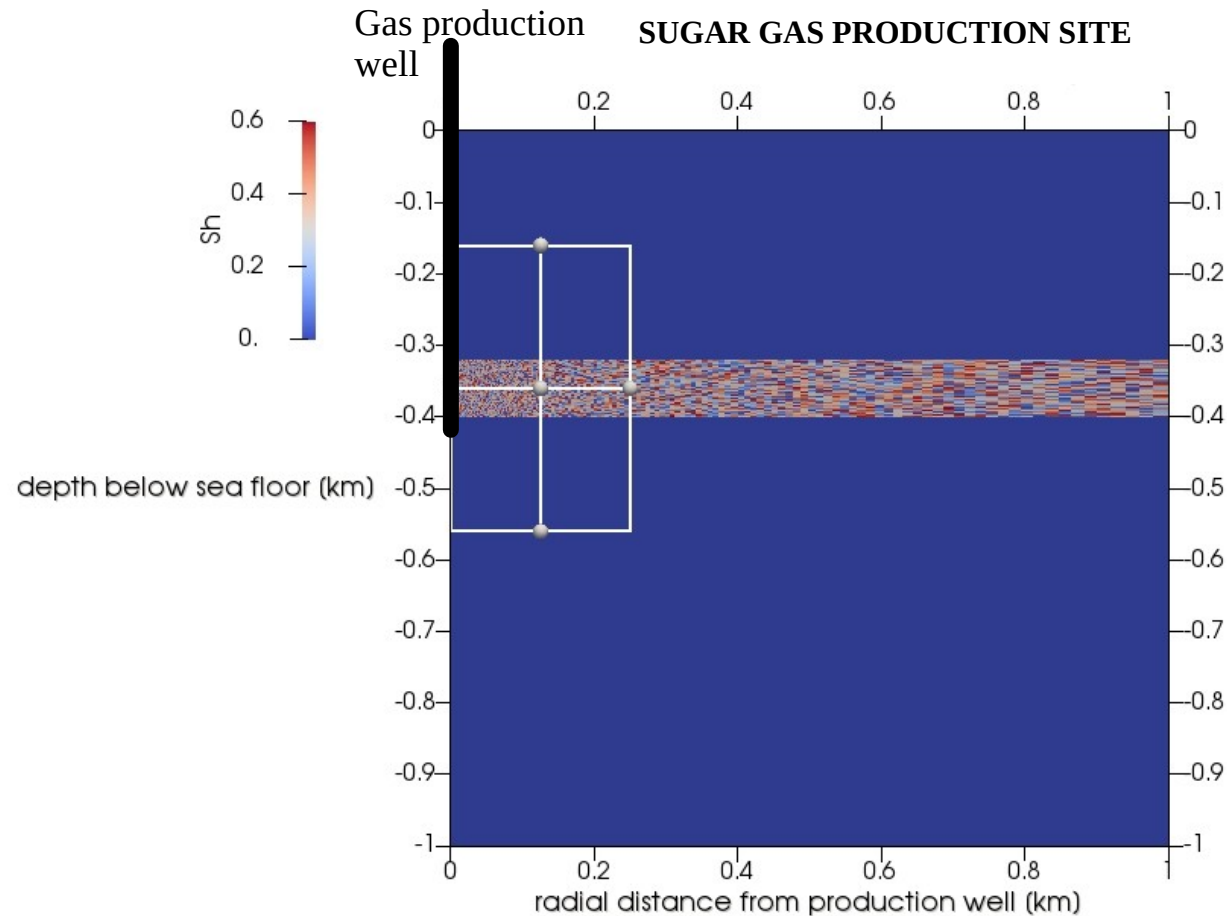


# Gas Production Example

## Single-well gas production scenario

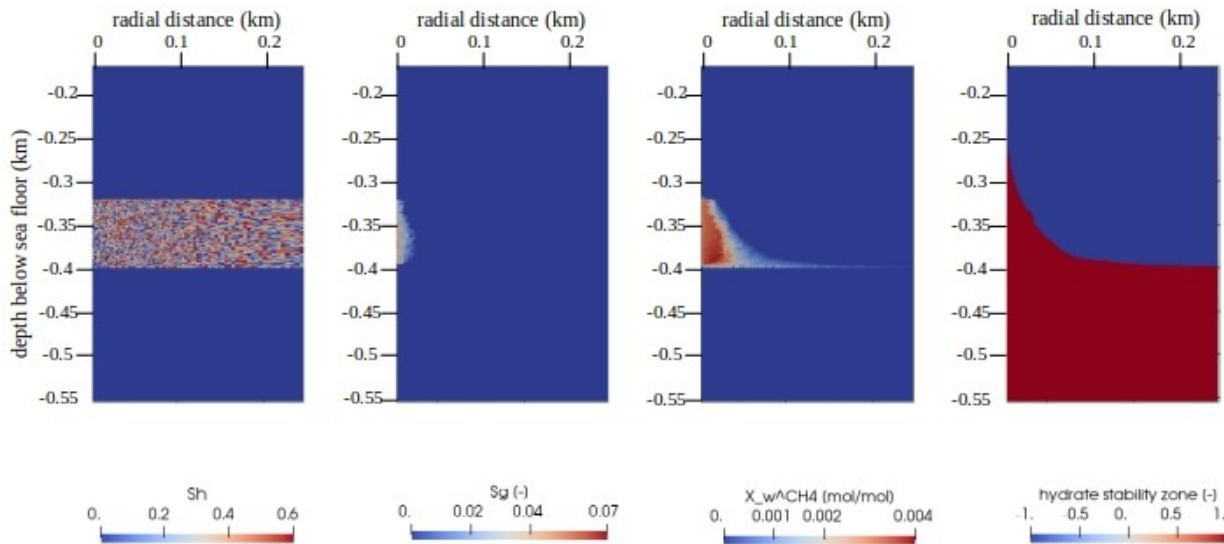
- Test setting based on the geological setting of the Black sea
- Random distribution of hydrate to test robustness of the scheme →  $S_h$  varies between **0 to 0.6**
- Corresponding abs. permeability ranges between  **$1.e-13$  to  $1.e-18$  m<sup>2</sup>**

Results

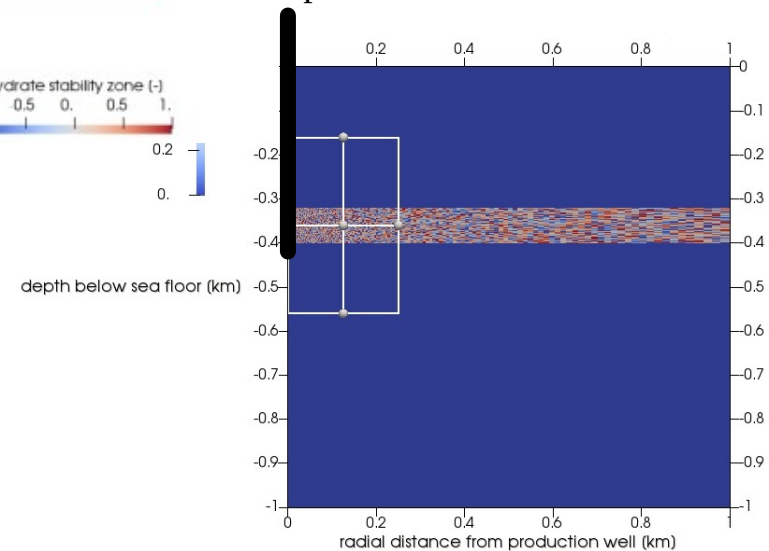


# Gas Production Example

$t = 10$  days



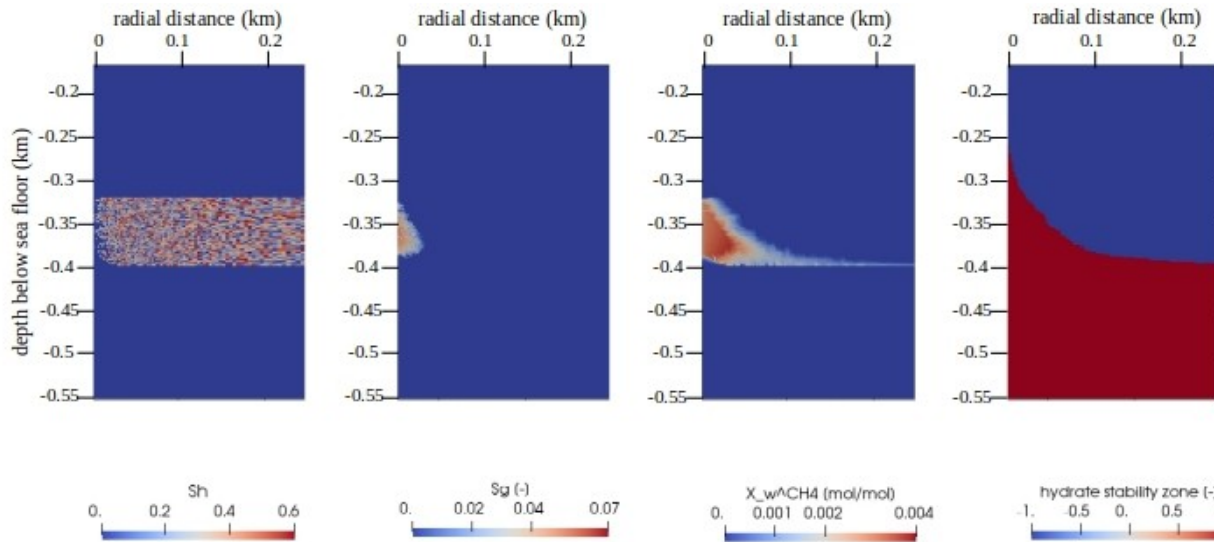
Gas production well



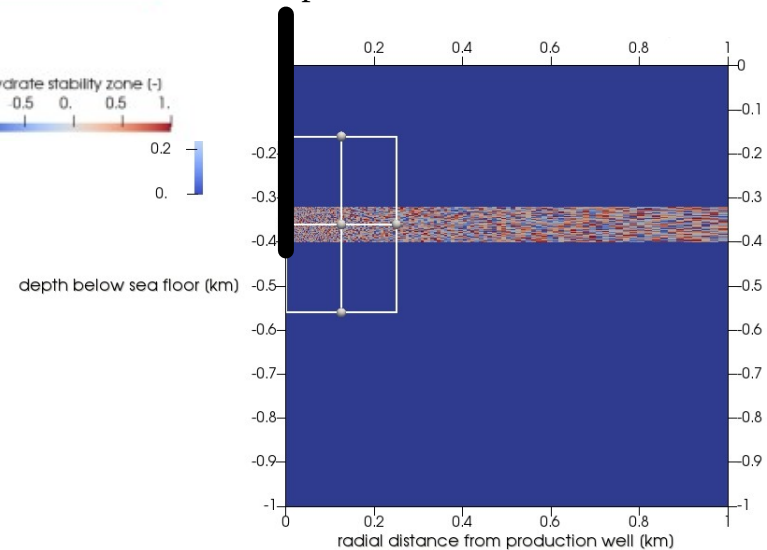


# Gas Production Example

t = 90 days

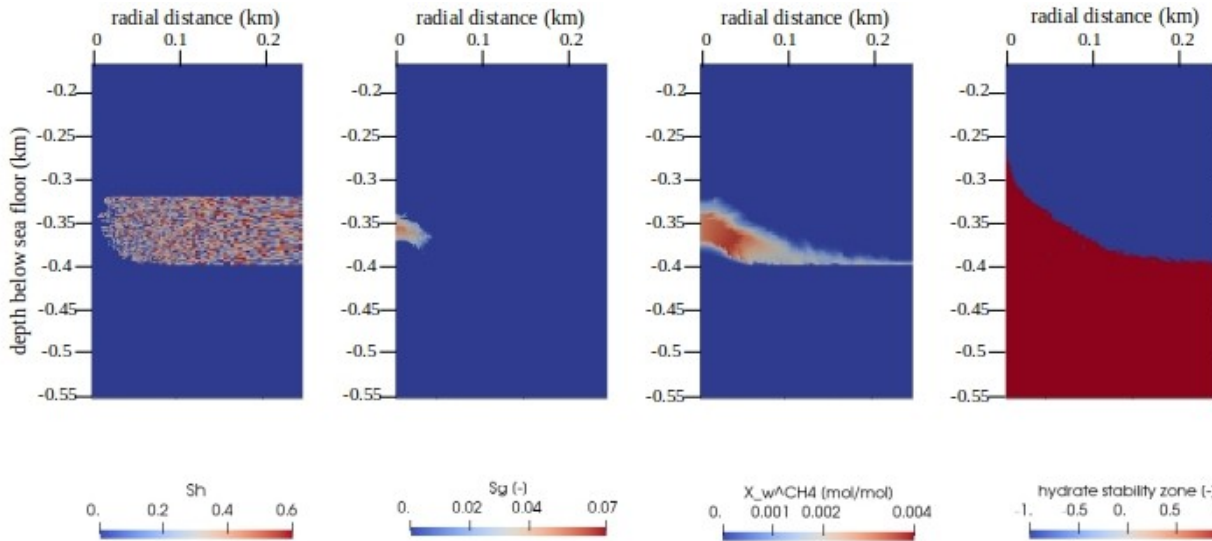


Gas production well

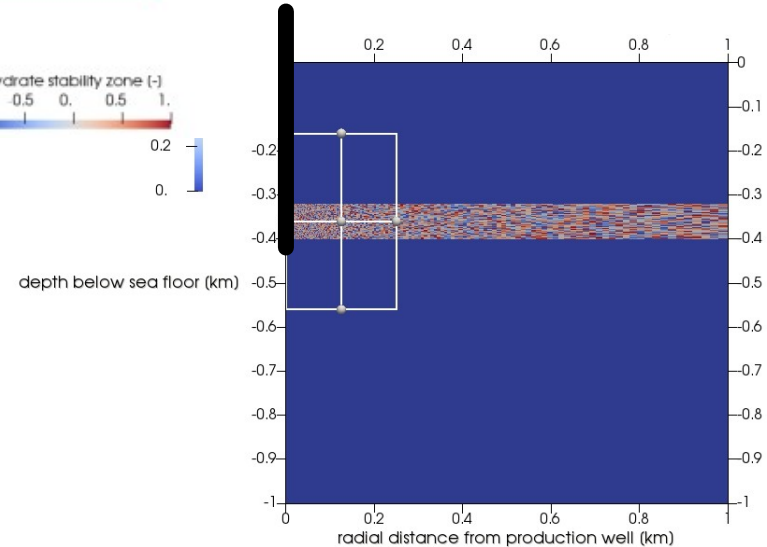


# Gas Production Example

t = 360 days



Gas production well



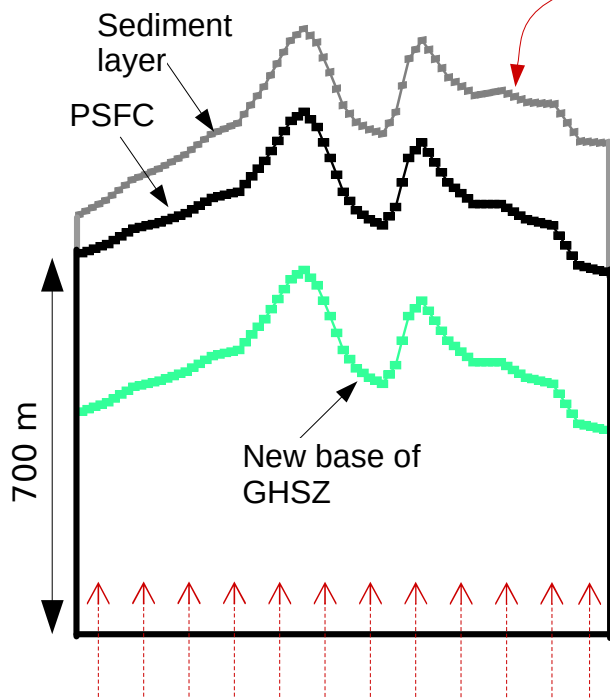
## References

---

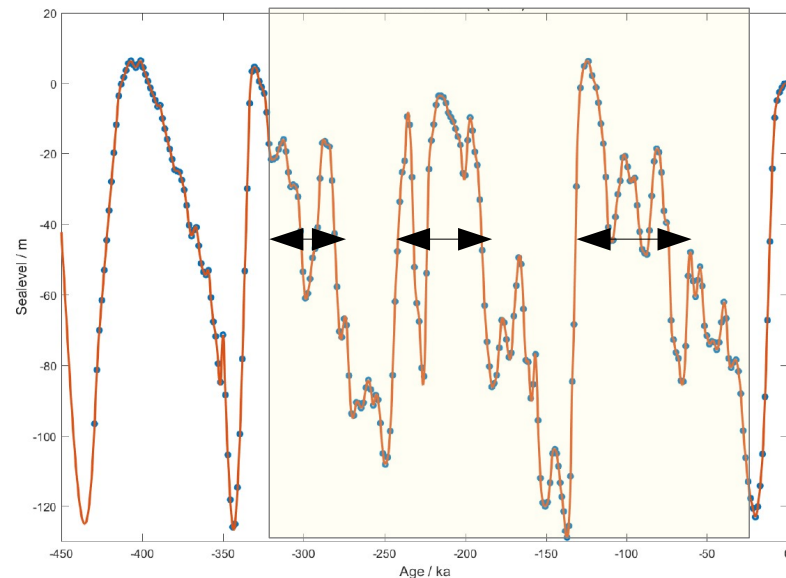
- Bastian, P., F. Heimann, and S. Marnach (2010), Generic implementation of finite element methods in the distributed and unified numerics environment (dune), *Kybernetika*, 46(2):294-315.
- Kim, H.C., P.R. Bishnoi, R.A. Heidemann, and S.S.H. Rizvi (1987), Kinetics of methane hydrate decomposition, *Chemical Engineering Science*, 42(7):1645-1653.
- Chaouachi, M., A. Falenty, K. Sell, F.Enzmann, M. Kersten, D. Habberthür, and W F. Kuhs (2015), Microstructural evolution of gas hydrates in sedimentary matrices observed with synchrotron X-ray computed tomographic microscopy, *Geochem. Geophys. Geosyst.*, 16:1711-1722.
- Das, A., A. Tengattini, G.D. Nguyen, G. Viggiani, S.A. Hall, and I. Einav (2014), A thermomechanical constitutive model for cemented granular materials with quantifiable internal variables. Part II - Validation and localization analysis, *Journal of the Mechanics and Physics of Solids*, 70(1):382405.
- Deusner, C., N. Bigalke, E. Kossel, and M. Haeckel (2012), Methane production from gas hydrate deposits through injection of supercritical CO<sub>2</sub>, *Energies*, 5(7):2112.
- Gupta, S., R. Helmig, and B. Wohlmuth (2015), Non-isothermal, multi-phase, multi-component flows through deformable methane hydrate reservoirs, *Computational Geo-sciences*, 19(5):1063-1088.
- Gupta, S., C. Deusner, M. Haeckel, R. Helmig, and B. Wohlmuth (2017), Testing a thermo-chemo-hydro-geomechanical model for gas hydrate-bearing sediments using triaxial compression laboratory experiments, *Geochem. Geophys. Geosyst.*, 18:3419-3437.
- Hager, C. (2010), Robust numerical algorithms for dynamic frictional contact problems with different time and space scales. PhD thesis, IANS, Universität Stuttgart.
- Kossel, E., N. Bigalke, E. Pinero, M. Haeckel (2013), The SUGAR Toolbox - A Library of Numerical Algorithms and Data for Modelling of Gas Hydrate Systems and Marine Environments, *GEOMAR Report Nr. 8*:160.
- Lauser, A., C. Hager, R. Helmig, B. Wohlmuth (2011), A new approach for phase transitions in miscible multi-phase flow in porous media, *Advances in Water Resources*, 34(8):957-966,
- Waite, W. F., W. J. Winters, and D. H. Mason (2004), Methane hydrate formation in partially water-saturated Ottawa sand, *Am. Min.*, 89(8-9):1202-1207.
- Zander, T., M. Haeckel, C. Berndt, W.C. Chi, I. Klauke, J. Bialas, D. Klaeschen, S. Koch, O. Atgn (2017), On the origin of multiple BSRs in the Danube deep-sea fan, Black Sea, *Earth and Planetary Science Letters*, 462:15-25.

Thank you for your attention !

# Further Field-Scale Studies

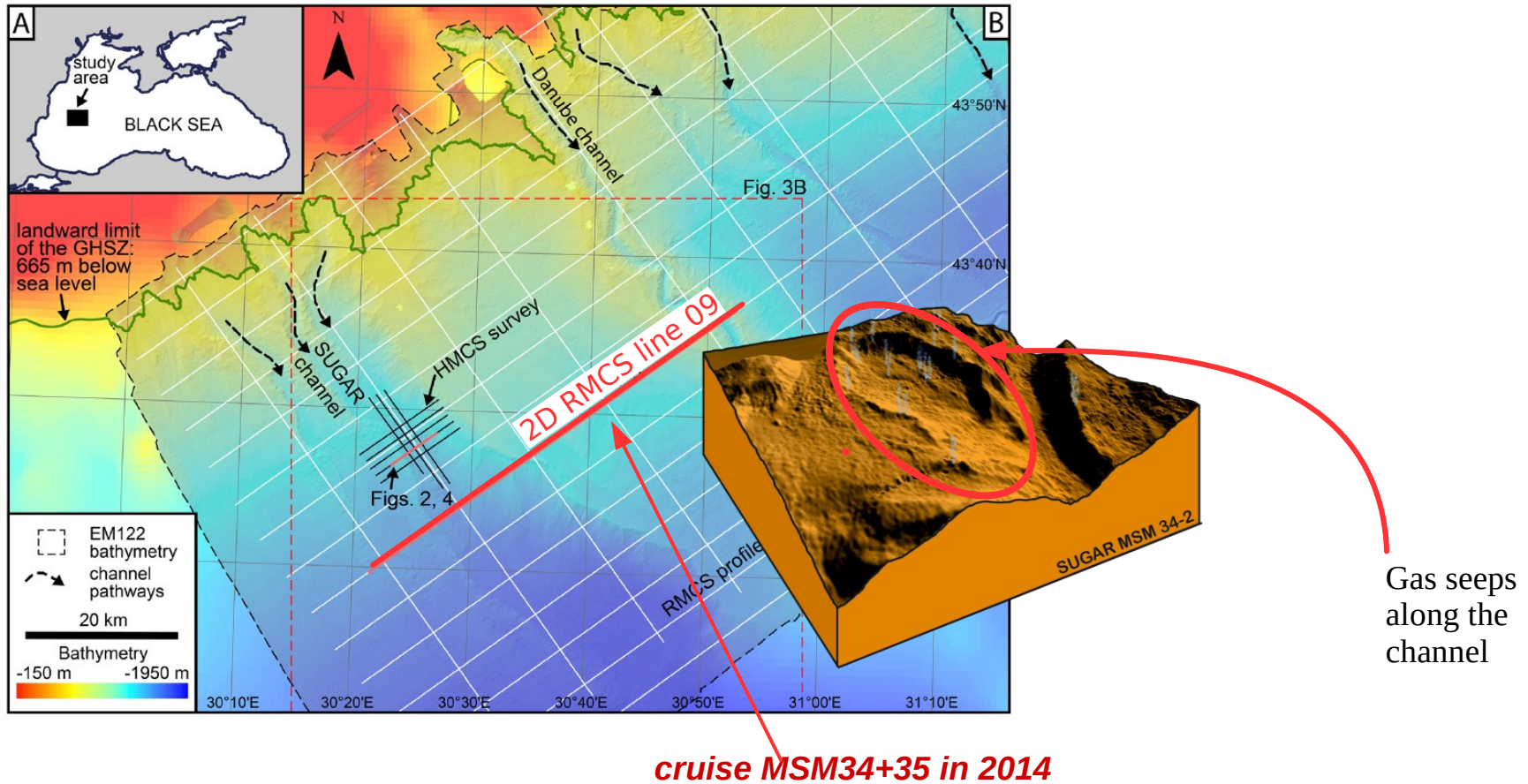


Depositional history [Waelbroek, 2002]



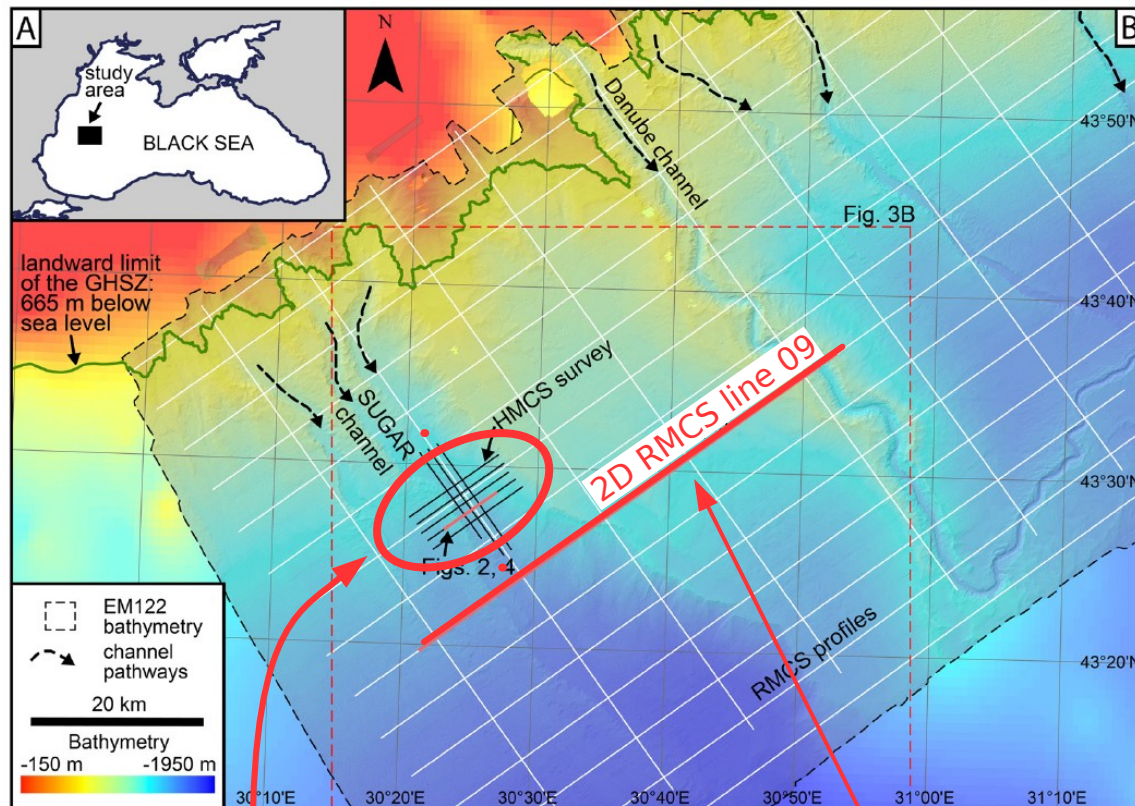
- Identify the **marine** and **limnic** stages
- Extrapolate deposition times and cut-off times from global water depths history

# Further Field-Scale Studies



## Further Field-Scale Studies

### SUGAR GAS PRODUCTION SITE

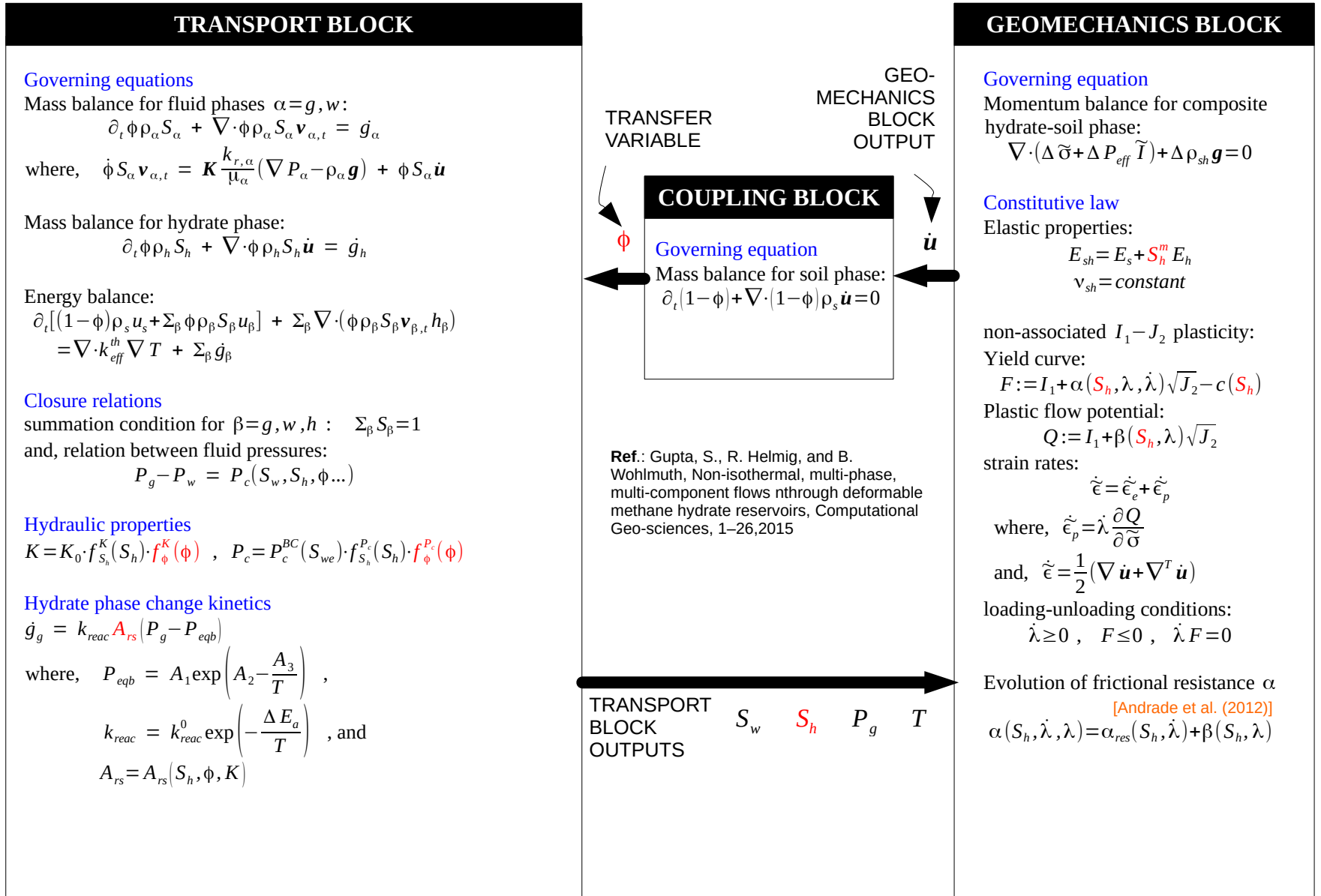


*research cruise M142 Dec. 2017*

*cruise MSM34+35 in 2014*

- simulate various *gas production scenarios* based on the geological setting of the gas hydrate reservoirs in the *paleo Danube deep-sea fan* in the Bulgarian sector of the Black Sea.
- slope stability/risk analyses.

# Mathematical Model





# Further Testing

## Drained triaxial experiments for calibration of plasticity model

- homogeneous gas hydrate distributions
- no hydrate phase change

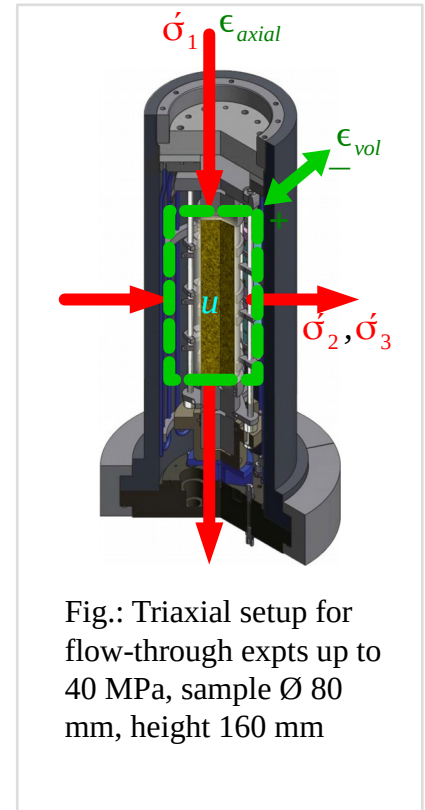
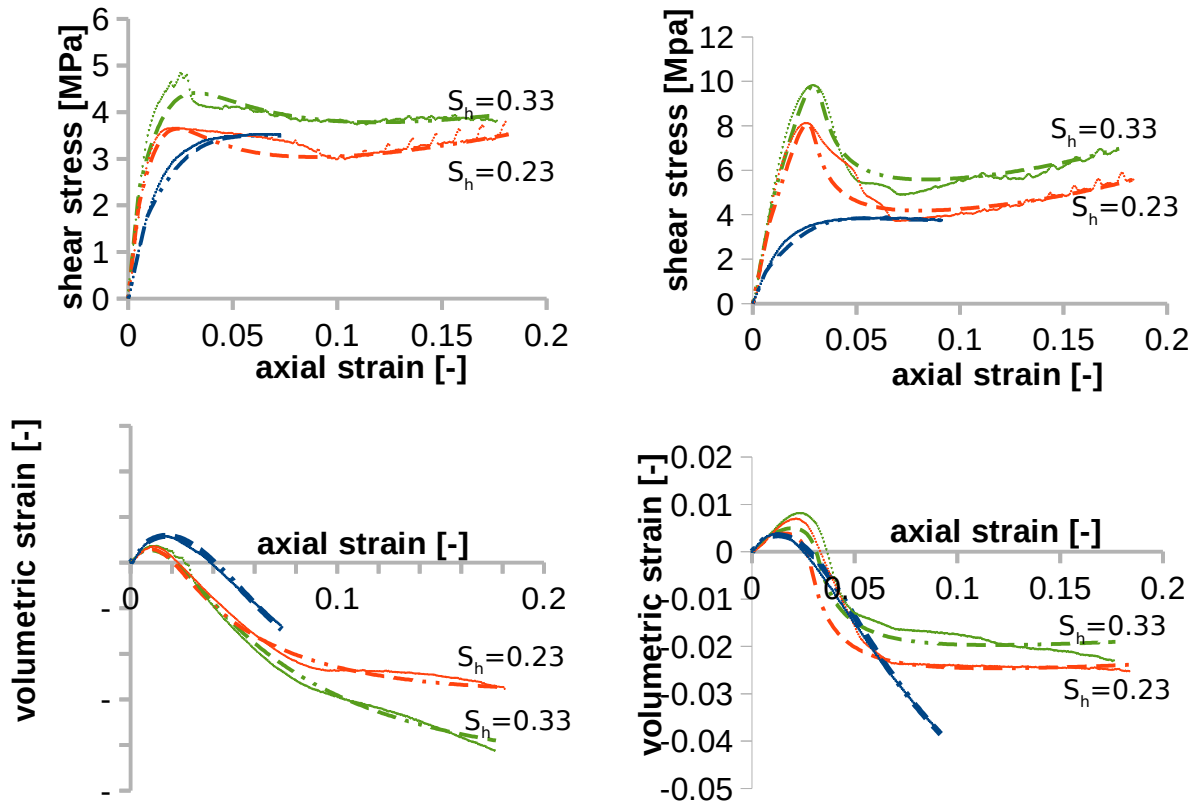


Fig.: Triaxial setup for flow-through expts up to 40 MPa, sample  $\varnothing$  80 mm, height 160 mm

**A. Water saturated samples,**  
Hydrates are formed through excess gas method.

**B. Gas saturated samples,**  
Hydrates are formed through excess gas method.

- experiment:  $S_h = 0$ .
- ◆ experiment:  $S_h = 0.23$
- ▼ experiment:  $S_h = 0.33$
- model:  $S_h = 0$ .
- model:  $S_h = 0.23$
- model:  $S_h = 0.33$

# Further Testing

## LAB-SCALE TEST

- advanced high-pressure flow-through triaxial set-up
- Heterogeneous gas hydrate distributions
- Coupled flow, hydrate phase change, and geomechanics

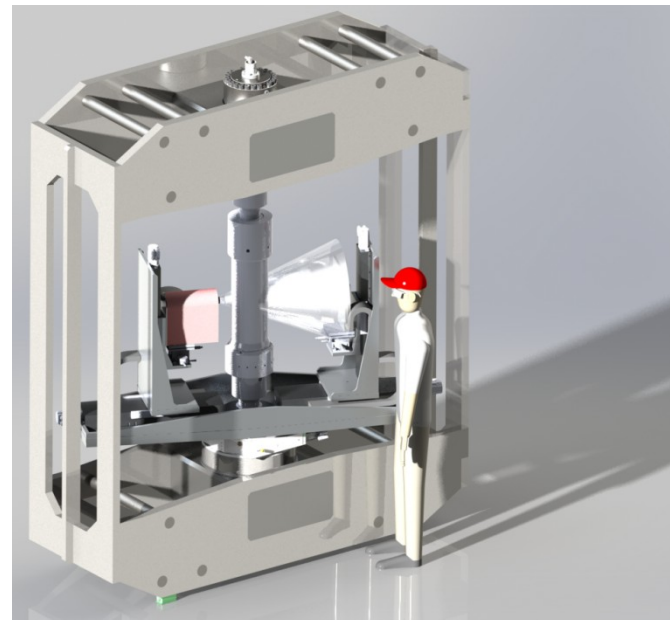
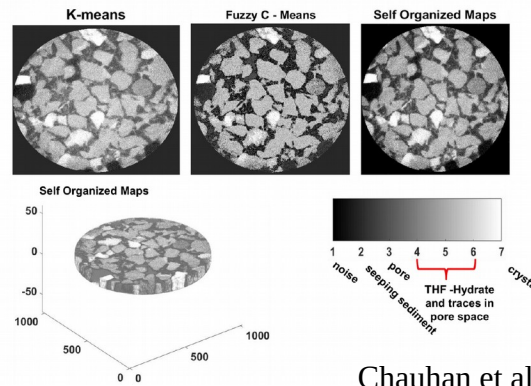


Fig.: XRAY-CT TRIAXIAL SET-UP